Generalization of Approximation of Planar Spiral Segments by Arc Splines

by

Lan Chen

A thesis

submitted to the faculty of graduate studies

in partial fulfillment of the requirements

for the degree of

Master of Science

Department of Computer Science

University of Manitoba

Winnipeg, Manitoba, Canada 1998

0-612-32073-1

THE UNIVERSITY OF MANITOBA

FACULTY OF GRADUATE STUDIES

*****

COPYRIGHT PERMISSION PAGE

GENERALIZATION OF APPROXIMATION OF PLANAR SPIRAL SEGMENTS BY ARC SPLINES

BY

LAN CHEN

A Thesis/Practicum submitted to the Faculty of Graduate Studies of The University of Manitoba in partial fulfillment of the requirements of the degree

of

MASTER OF SCIENCE

Abstract

Spirals based on quadratic Bézier, cubic Bézier, Pythagorean hodogragh (PH) cubic, PH quintic and clothoid curves are suitable for CAD and computer-aided geometric design (CAGD) applications. The clothoidal spiral segments are widely used in highway design, railway design and robot trajectories. For CNC machining compared with polyline approximations, the suggested arc spline approximations avoid sudden changes in the direction of the tool path, decrease the number of segments for approximation and lessen the need to polish objects. In this dissertation an existing method is generalized to approximate a planar spiral segment so that it can be applied to a large class of spiral segments. The properties of several spiral segments are analyzed and their approximations by the proposed method are presented.

Acknowledgements

I would like to thank my advisor Dr. Desmond Walton who has provided me with guidance, advice, encouragement, and support throughout my Master studies. I wish to thank the members of my committee, Dr. D. Meek and Dr. W. Hoskins for reading the thesis and offering invaluable advice to me.

I would like to take this opportunity to give a special thanks to my dear friends. I would like to thank my parents, sisters for their constant love and support.

Contents

List of Figures

List of Tables

Chapter 1

Introduction

With the influence of automatic control of machines and computer-aided design (CAD), computer-aided manufacturing (CAM) systems have expanded in manufacturing industries during the last two or three decades. Designers use CAD systems to design parts for visual and theoretical analysis. On the basis of the CAD model. the numerical control (NC) programmer uses the CAM system to generate a NC tool path for a computerized numerical control (CNC) machine so that it can produce the part. Approximating spirals by arc splines plays an important role in CNC machining for manufacture.

Spirals based on quadratic Bézier, cubic Bézier, Pythagorean hodogragh (PH) cubic, PH quintic and clothoid curves are suitable for CAD and computer-aided geometric design (CAGD) applications. PH curves were introduced by Farouki and Sakkalis [FS90]. Spiral segments, the clothoid in particular, are used in applications such as highway design [Baa84], railway design [Hic67] and robot trajectories [Sch96].

The term spline is used to describe a composition of curve segments joined in a manner to satisfy given continuity and smoothness criteria. A spline function (or a spline curve) is a piecewise analytical function. The different pieces are chained together with continuity requirements imposed on the first few derivatives at the joints. The pieces are basic curve shapes with adjustable parameters. The parameters are adjusted so that the chained curve matches the data and continuity requirements. For example, an arc spline is a spline composed of circular arcs.

A CNC machine is a piece of manufacturing equipment that performs machining automatically to produce parts. The tool paths of modern CNC manufacturing machines are controlled by servomotors which allow circular arcs and straight line segments to be machined to almost mathematical precision. In a CAD environment, objects are often designed using B-splines or Bézier curves. It is standard practice to cut a smooth curve as a polygon that is a very close approximation to the curve. To manufacture computer-aided designed objects, efficient and effective use of such machines can be increased by approximating Bézier and B-spline curve segments by arc splines rather than by straight line segments for the following reasons.

- The continuity of the tangent vector of an arc spline avoids sudden changes in the direction of the tool path. Sudden changes of direction cause problems such as overshooting. Such problems lead to wastage of material and time, or shuddering of the machine. These problems result in increased maintenance costs and a shorter lifespan for costly equipment. To avoid overshooting, programming of the feedrate, acceleration and deceleration should be done carefully and is usually very time-consuming.

- The number of segments in the approximation will be decreased which leads to fewer instructions and fewer tool motions required in programming the machine.

- The need to polish objects would be significantly reduced if they were machined with a continuous tangent cutting path.

1.1 Notation, Conventions and Terminology

In this thesis the concepts of a vector, the norm of a vector and its dot and cross products are used. The spirals and spiral segments discussed are planar curves, however it may be necessary to refer to a curve or vector in space. Some of the properties of vectors are mentioned here. More details are available in [dC76] and [Gug63].

Norm of a Vector :

The norm of a vector $\mathbf{V}$ is denoted as $\| \mathbf{V} \|$. If $v = (v_1, v_2, v_3)$, then

$$\| \mathbf{V} \| = \sqrt{v_1^2 + v_2^2 + v_3^2}.$$

Angle :

The angle from vector $\mathbf{U}$ to vector $\mathbf{V}$ is a signed quantity; it is positive if measured counter-clockwise from $\mathbf{U}$ to $\mathbf{V}$.

Directed Line Segment :

The directed-line segment from point $\mathbf{P}_i$ to point $\mathbf{P}_j$ is indicated as $\mathbf{P}_i\mathbf{P}_j$. The length (norm) of it is denoted as $\| \mathbf{P}_i\mathbf{P}_j \|$.

Parameterized Curve :

A three dimensional curve is denoted as $(x(t), y(t), z(t))$. The quantity t is called the parameter of the curve. The degree of smoothness of a parameterized curve depends on how many times it can be differentiated. For planar curves, $z(t) = 0$.

Dot Product :

The dot (or inner) product of two vectors, $\mathbf{V}$ and $\mathbf{W}$ is denoted as $\mathbf{V} \cdot \mathbf{W}$. It is defined by

$$\mathbf{V} \cdot \mathbf{W} = \| \mathbf{V} \| \| \mathbf{W} \| \cos\theta,$$

where θ is the counter-clockwise angle from vector $\mathbf{V}$ to vector $\mathbf{W}$. The following are some properties of the dot product [dC76]:

1. Assume $\mathbf{V}$ and $\mathbf{W}$ are two nonzero vectors, the necessary and sufficient condition for $\mathbf{V} \cdot \mathbf{W} = 0$ is that $\mathbf{V}$ and $\mathbf{W}$ be orthogonal.
2. $\mathbf{V} \cdot \mathbf{W} = \mathbf{W} \cdot \mathbf{V}$.
3. $\lambda(\mathbf{V} \cdot \mathbf{W}) = \lambda\mathbf{V} \cdot \mathbf{W} = \mathbf{V} \cdot \lambda\mathbf{W}$.
4. $\mathbf{U} \cdot (\mathbf{V} + \mathbf{W}) = \mathbf{U} \cdot \mathbf{V} + \mathbf{U} \cdot \mathbf{W}$.

Let $\mathbf{e}_1 = (1, 0, 0), \mathbf{e}_2 = (0, 1, 0)$ and $\mathbf{e}_3 = (0, 0, 1)$. Using property 1, it is easy to see that $\mathbf{e}_i \cdot \mathbf{e}_j = 1$ if $i = j$ otherwise $\mathbf{e}_i \cdot \mathbf{e}_j = 0$. Suppose

$$\mathbf{U} = u_1\mathbf{e}_1 + u_2\mathbf{e}_2 + u_3\mathbf{e}_3, \quad \mathbf{V} = v_1\mathbf{e}_1 + v_2\mathbf{e}_2 + v_3\mathbf{e}_3.$$

From properties 3 and 4, $\mathbf{U} \cdot \mathbf{V} = u_1v_1 + u_2v_2 + u_3v_3$. If $\mathbf{u}(t)$ and $\mathbf{v}(t)$ are differentiable functions, then the dot product of $\mathbf{u}(t)$ and $\mathbf{v}(t)$ is a differentiable function,

$$\frac{d}{dt}(\mathbf{u}(t)\cdot\mathbf{v}(t)) = \mathbf{u}'(t)\cdot\mathbf{v}(t) + \mathbf{u}(t)\cdot\mathbf{v}'(t).$$

Arc Length :

According to [dC76] (p. 6), the arc length of a regular parameterized curve from the point t_0 to t is

$$s(t) = \int_{t_0}^{t} \| \mathbf{Q}'(t) \| \, dt,$$

where

$$\| \mathbf{Q}'(t) \| = \sqrt{(x'(t))^2 + (y'(t))^2 + (z'(t))^2}$$

is the length of the vector $\mathbf{Q}'(t)$.

Unit Tangent Vector :

If the parametric curve $\mathbf{Q}(t)$ is considered to be the path of motion of a point. the direction of the first derivative vector gives the direction of motion and speed of the point at any instant. The direction is extracted from a parametric first derivative by normalizing the vector. The unit tangent vector of a curve $\mathbf{Q}(t)$ is

$$\mathbf{T}(t) = \frac{\mathbf{Q}'(t)}{\| \mathbf{Q}'(t) \|}.$$

If $\mathbf{T}$ is the unit tangent vector to $\mathbf{Q}(t)$ at t, then the orientation of the unit vector measured $\frac{\pi}{2}$ counter-clockwisely from $\mathbf{T}$ is the unit normal vector, denoted as $\mathbf{N}$.

Curvature : The curvature of a planar curve $\mathbf{Q}(t)(x(t), y(t))$ [?](p. 155) is

$$\frac{x'(t)y''(t) - y'(t)x''(t)}{\| \mathbf{Q}'(t) \|^3}. \tag{1.1}$$

The radius of curvature is the absolute value of the reciprocal of (1.1). At a given point **P** on a parametrically defined curve $\mathbf{Q}(t)$, the circle that passes through **P**, and at **P** has the same unit tangent vector and curvature as the curve, is called the osculating circle at **P**. The center and radius of this circle are called the center of curvature $\mathbf{C}(t)$ and the radius of curvature $\rho(t)$, respectively, at this point. The curvature $\kappa(t)$ at this point is the reciprocal, $1/\rho(t)$, of the radius of curvature. Here $\rho(t) \neq 0$. Otherwise, the curvature were infinite which contradicts with that curvature can always be measured in real world. The curvature vector **k** has a magnitude equal to the curvature and points from **P** towards the center of curvature.

Inflection Point :

An inflection point on a curve is defined as a point, **I**, where the points immediately before and after it are on opposite sides of the tangent line to the curve through the point **I** as in Fig. (1.1).

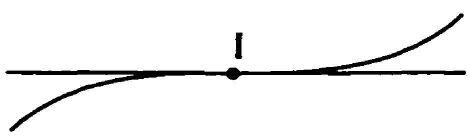

Figure 1.1: Inflection Point

$\mathbf{G}^0$ *continuity* :

Two curve segments are said to be joined with $\mathbf{G}^0$ continuity if one segment begins where the other segment ends.

$\mathbf{G}^1$ *continuity* :

Two curve segments are said to be joined with $\mathbf{G}^1$ continuity if they meet with $\mathbf{G}^0$ continuity and the tangent vectors at the joint between two these successive segments are collinear having the same direction.

$\mathbf{G}^2$ *continuity* :

Two curve segments are said to be joined with $\mathbf{G}^2$ continuity if they meet with $\mathbf{G}^1$ continuity and their signed curvatures are continuous across the joint.

Spiral :

Spirals are curves whose curvature is a monotonic function of arc length. In this thesis only spirals with positive curvature are considered. Results for spirals with negative curvature follow analogously. Consider a spiral $\mathbf{Q}(\mathrm{t})$ with parameter t, which increases strictly monotonically with arc length. The spiral $\mathbf{Q}(\mathrm{t})$ satisfies the following properties.

- The curvature at the first point of the spiral cannot be the same value as the curvature at the last point of the spiral.
- The spiral is a function of t.

Spirals, in which the absolute value of curvature increases, are denoted as winding spirals. Spirals, in which the absolute value of curvature decreases are denoted as unwinding spirals.

In this thesis, only continuous arc splines with first derivative continuity will be considered for approximating spiral segments. The first derivative at any point of such curves is not zero. The parameter t can range from $-\infty$ to $+\infty$ for some spirals, e.g. clothoidal, Archimedean and logarithmic spirals. To approximate a spiral with parameter t ranging from $-\infty$ to $+\infty$ by using the method illustrated in this thesis, the spiral should be separated into pieces with finite intervals. Using the same tolerance, different separations usually lead to different numbers of circular arcs. Only winding spirals are considered. The results are applicable to unwinding spirals by reversing the direction of the parameter.

Definition of Bézier curve :

The Bernstein Bézier curve [BBB87], or more briefly Bézier curve, of degree n is defined by:

$$\mathbf{Q}(t) = \sum_{i=0}^{n} \mathbf{P}_i C_{i,n}(t) \quad \text{for } 0 \le t \le 1, \tag{1.2}$$

where

$$C_{i,n}(t) = \begin{pmatrix} n \\ i \end{pmatrix} t^i (1-t)^{n-i}$$

are the Bernstein polynomials, the $\begin{pmatrix} n \\ i \end{pmatrix}$ being the binomial coefficients and $\mathbf{P}_i$ are the control vertices. $\mathbf{P}_0, \mathbf{P}_1, \cdots, \mathbf{P}_n$ form the control polygon.

The first derivative is

$$\mathbf{Q}'(t) = n \sum_{i=0}^{n-1} \begin{pmatrix} n-1 \\ i \end{pmatrix} (\mathbf{P}_{i+1} - \mathbf{P}_i)(1-t)^{n-i-1} t^i, \quad \text{for } 0 \le t \le 1. \tag{1.3}$$

Some useful properties of Bézier curves are:

- Convex-hull property:

  A Bézier curve lies within the convex hull of its control polygon. The convex hull of a set of control vertices in the plane can be thought of as the region lying inside a rubber band stretched so as to contain the control vertices and then released so that it snaps tightly against them.

- Endpoint interpolation:

$$\mathbf{Q}(0) = \mathbf{P}_0 \quad \mathbf{Q}(1) = \mathbf{P}_n.$$

- The tangent vectors at the starting point and ending point are parallel to the beginning and ending edges of the control polygon, i.e.:

$$\mathbf{Q}'(0) = n(\mathbf{P}_1 - \mathbf{P}_0) \quad \mathbf{Q}'(1) = n(\mathbf{P}_n - \mathbf{P}_{n-1})$$

respectively.

- The curvature at the starting point and ending point depend on only the first three or last three control points because

$$\mathbf{Q}''(0) = n(n-1)[(\mathbf{P}_2 - \mathbf{P}_1) - (\mathbf{P}_1 - \mathbf{P}_0)]$$

$$\mathbf{Q}''(1) = n(n-1)[(\mathbf{P}_{n-2} - \mathbf{P}_{n-1}) - (\mathbf{P}_{n-1} - \mathbf{P}_n)]$$

Spiral Segment :

A spiral segment is a piece of any spiral. Curvature extrema and inflection points divide divide a general curve into spiral segments.

Arc Spline :

An arc spline is a $\mathbf{G}^1$ curve composed of circular arcs and straight line segments. First-order geometric continuity, denoted as $\mathbf{G}^1$, refers to a continuous spline with a continuously varying unit tangent vector. Arc splines are $\mathbf{G}^1$ continuous, but not $\mathbf{G}^2$ continuous, because their unit tangent vectors vary continuously but their curvature at the joints are not continuous.

Biarc :

Consider two given arbitrary points $\mathbf{A}_0$ and $\mathbf{A}_1$ and corresponding tangent directions $\mathbf{T}_0$ and $\mathbf{T}_1$. A biarc is a composition of two circular arcs that satisfy the following:

- One arc starts at $\mathbf{A}_0$ with tangent vector $\mathbf{T}_0$ at $\mathbf{A}_0$.
- The other arc ends at $\mathbf{A}_1$ with tangent vector $\mathbf{T}_1$ at $\mathbf{A}_1$.
- The two arcs are connected at a joining point, $\mathbf{P}$, at which they have a common unit tangent vector.

There are two types of biarcs: those that have an inflection point (as shown in Fig. (1.2) and those that do not have an inflection point (as shown in Fig. (1.3)).

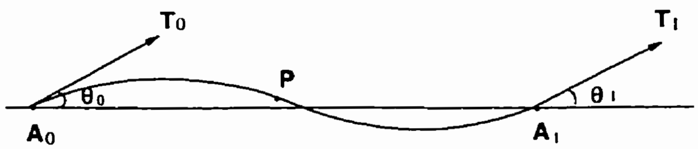

Figure 1.2: Curve with Inflection Point

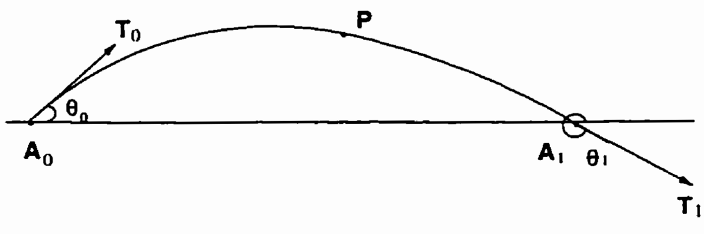

Figure 1.3: Curve without Inflection Point

PH curve :

A Pythagorean hodograph (PH) curve is a polynomial parametric curve

$$\mathbf{Q}(t) = (x(t), y(t))$$

where $x'(t)^2 + y'(t)^2$ can be expressed as the square of a polynomial in t. More details on PH curves are in Chapter 2.

1.2 Literature Review

In this thesis, all of the spirals discussed are plane curves which are special cases of space curves. For a space curve in general, denote the unit tangent of a curve $\mathbf{Q}(t)$ as $\mathbf{T}(t)$ and the normal of $\mathbf{Q}(t)$ as $\mathbf{N}(t)$. The osculating plane at t is determined by these two vectors. The unit vector $\mathbf{B}(t) = \mathbf{T}(t) \times \mathbf{N}(t)$ is normal to the osculating plane (see Fig. (1.4)). The number $\tau(t)$ defined by $\mathbf{B}'(t) = \tau(t)\mathbf{N}(t)$ is called the torsion of $\mathbf{Q}$ at t [dC76]. For a planar curve $\tau = 0$ and it is possible to give the curvature a sign when the curvature is compared with the orientation of the plane. The curvature changes sign when either the orientation of the curve or the orientation of the plane is changed. This is called signed curvature.

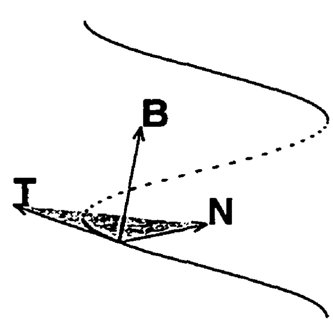

Figure 1.4: General Space Curve

In [Meh74] on nonlinear splines Mehlum concludes that it is possible to approximate any planar curve by a sequence of circular arcs for given accuracy and continuity requirements. In his paper, Mehlum describes a theory of nonlinear splines arising from a variational criterion of the type

$$\int (curvature)^2 ds = \text{“as little as possible”}$$

He proves that the curvature varies linearly along some fixed direction in space when $\tau = 0$. Based on the special case $\tau = 0$, some algorithms for curve fitting are shown. Mehlum in fact encountered the clothoid and described an arc spline approximation to it. His arc spline approximation is based on a differential equation that he encountered and is thus particular to his approximation of a non-linear spline.

In Walton and Meek's paper [WM94], a simple technique is developed to find an arbitrarily close approximation to a quadratic Bézier by a $\mathbf{G}^1$ curve consisting of circular arcs. A quadratic Bézier is in general not a spiral segment; it may or may not have a local curvature maximum. It can have at most one local curvature maximum. When it does not have an interior curvature maximum, it is a spiral segment. A quadratic Bézier is given by

$$\mathbf{Q}(t) = \mathbf{P}_0(1-t)^2 + 2\mathbf{P}_1(1-t)t + \mathbf{P}_2 t^2, \quad 0 \le t \le 1, \tag{1.4}$$

where $\mathbf{P}_0, \mathbf{P}_1, \mathbf{P}_2$ are distinct and non collinear control vertices. Three theorems are presented in that paper. The first theorem is useful in the construction of a biarc approximation to a quadratic Bézier curve. The other two theorems are useful to measure the accuracy of the approximation. *Theorem* 1 of [WM94] states:

A unique biarc can be constructed which satisfies the following conditions.

- *The biarc is C-shaped and matches the quadratic Bézier curve in position and tangential directions at* $\mathbf{P}_0$ *and* $\mathbf{P}_2$.
- *The tangential direction at the joint of the biarc matches the direction of the line segment which joins* $\mathbf{P}_0$ *to* $\mathbf{P}_2$.
- *The biarc lies in the convex hull defined by* $\mathbf{P}_0, \mathbf{P}_1, \mathbf{P}_2$.

Theorem 2 of [WM94] gives the corresponding parameter t where the deviation reaches the maximum value. In the same article, *Theorem* 3 finds the maximum deviation from the biarc, as constructed in *Theorem* 1, measured along a radial direction of the biarc. An algorithm is developed to approximate a quadratic Bézier within a given tolerance by subdividing it recursively.

In Walton and Meek's paper [WM96c], a technique which is similar to the one used for a quadratic Bézier segment is applied to a planar cubic Bézier segment and two theorems on the deviation of a biarc approximation from a segment of the cubic Bézier spiral segment are presented.

Meek and Walton's paper [MW95] presents an algorithm for finding an arbitrarily close arc spline approximation of a smooth curve by examining the family of circular arcs joining one given point $\mathbf{A}_0$ to another distinct given point $\mathbf{A}_1$. The two circular arcs that match a given unit tangent vector $\mathbf{T}_0$ at the first point and that match a given unit tangent vector $\mathbf{T}_1$ at the second point $\mathbf{A}_1$ are called the bounding circular arcs C_0 and C_1 (see Fig. (1.5)).

Theorem 2 of [MW95] states that any biarc that joins one point to another distinct point and matches given unit tangent vectors at the two points lies between the bounding circular arcs that are derived from the two points and the two unit tangent

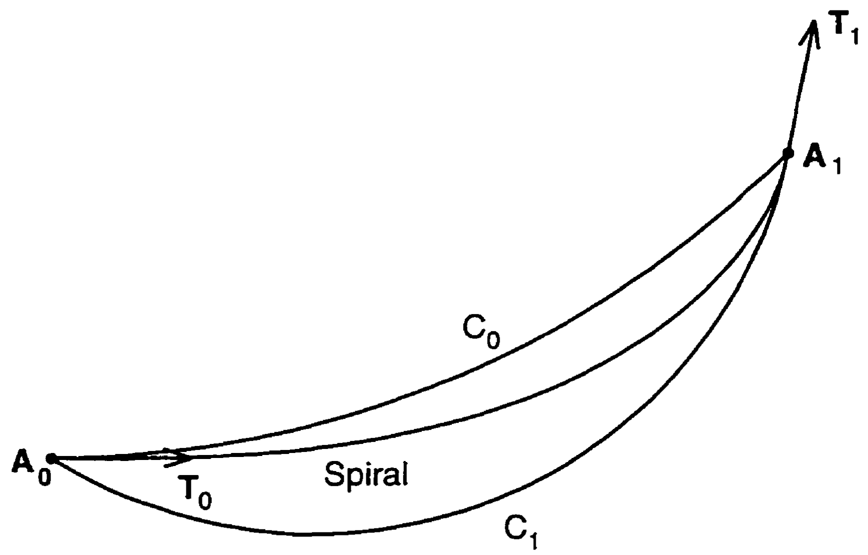

Figure 1.5: Bounding Circular Arcs

vectors. *Theorem* 5 of [MW95] shows that if a convex spiral segment of positive increasing curvature satisfies the enclosing condition, then the bounding circular arcs enclose a crescent-shaped region that includes the entire spiral segment. Based on these two theorems, *Theorem* 6 of [MW95] is deduced which states the following.

> *Let* $\mathbf{Q}(t)$, $t_0 \leq s \leq t_1$, *be a smooth spiral segment of positive increasing curvature for which the derived bounding circular arcs have curvatures of the same sign, then the maximum distance between the two bounding circular arcs is* $\mathbf{O}(h^3)$, *where* $h = t_1 - t_0$.

The algorithm used in this method is also a recursive one. Suppose $\mathbf{A}_0$ and $\mathbf{A}_1$ are the points on the curve to be approximated; if $\mathbf{A}_0$ and $\mathbf{A}_1$ are very close, a straight line is returned as part of the arc spline approximation, otherwise check if the condition of *Theorem* 5 is satisfied. If it is satisfied, a biarc is fitted, otherwise the curve is subdivided. Since this method can be used on any spiral segment, it can be called a generalized one. This method causes some unnecessary subdivision. In this thesis a more refined method of deviation calculation is used and it requires substantially less resources. It cannot be claimed that the methods used in this thesis are optimal. However, they seem to produce a good ratio of maximum deviation to specified tolerance. Referring to [WM96c], for example, using the method of [MW95] on a cubic spiral segment produced 16 arcs with a maximum distance between bounding arcs of 0.001632 but a maximum deviation of 0.0001599, and 32 arcs with a maximum distance between bounding arcs of 0.0002072 but a maximum deviation of 0.00001992, i.e. ratios of 0.0980 and 0.0961, respectively. On the other hand, when 0.001632 and 0.0002072 were specified as tolerances, the algorithm discussed in [WM96c] produced 10 and 18 arcs with maximum deviations of 0.001431 and 0.0001933 for ratios of 0.877 and 0.933, respectively.

Another approximation of spirals by arc splines is discussed in [MP84]. In that paper, Marciniak and Putz develop an algorithm to approximate plane spirals by smooth piecewise circular arc splines using the fewest segments within a given tolerance. The method they provide is for solving the problem of spiral approximation by tangent-continuous curves composed of circular arcs. It has the following properties:

1. The approximation is within a given deviation of the given spiral, measured along the normal to the spiral.

2. The approximation is optimal in the sense that it has the fewest circular arc segments among those with a given deviation.

The method can be described as follows:

For a spiral $K(t)$, where $t \in [t_0, t_k]$ and τ is an allowable tolerance, an internal spiral is defined as $K_i(t)$, where $t \in [t_0, t_k]$ and an external spiral is defined as $K_e(t)$,where $t \in [t_0, t_k]$. The distance from the spiral to either the internal one or the external one, equals τ. The approximating curve must lie in an area of tolerance delimited by internal and external spirals. The approximating curve consists of the first circular arc segment and a number of sequential circular arc segments. The first circular arc has four points in common with the spirals that delimit the tolerance field. Each sequential arc has three points in common with these limiting spirals. The common points alternate between the limiting spirals. The error of approximation, measured along the normal to the spiral, attains its maximal value τ with alternating sign.

An algorithm which solves this problem, and an example of its application for any curve is presented in [MP84]. The approximation does not match the beginning and ending points and tangential directions of the spiral segments. If a design involves two spirals intended to be joined smoothly, this smooth blend is not incorporated in the arc spline approximation. For a corresponding toolpath there may thus be sudden changes in the position and direction of the machine tool at the joints. A comparison is made in Chapter 3 between the method of [MP84] and the one used in this thesis.

1.3 Approximation of Spiral Segments

Usually general methods are not as efficient as specialized methods. It is interesting to know if the specialized methods mentioned in Section (1.2) can be generalized to a larger class of spirals while retaining efficiency, e.g. can the same technique used for quadratic and cubic Bézier spiral segments be generalized for other polynomial spirals? Can it be applied to other spirals?

Since the quadratic and cubic Bézier can be approximated by using that method, it is expected that other spirals may be approximated by arc splines using a similar technique. In this thesis, the PH cubic Bézier, PH quintic Bézier, clothoidal, Archimedean and logarithmic spirals are examined in order to develop a general algorithm for their approximation by arc splines.

In general the spiral segments which are investigated in this thesis have the rotation of the tangent from one end to the other that is smaller than π. For some spiral segments this angle can not reach π because of the limitation of the curve itself, e.g. the spiral part of a parabola. A spiral segment of the class examined in this thesis lies within the triangle formed by its endpoints, and the intersection of the straight lines which pass through its endpoints and are parallel to the tangential directions of the segment at its endpoints. A spiral where the rotation of tangent is greater than or equal to π can be approximated by subdividing it into segments and approximating each segment separately.

In Chapter 2 some theoretical background which is relevant to this thesis is introduced. Spirals which are approximated in this thesis are defined and some properties of them are mentioned . In Chapter 3, two main theorems are presented and proved to show the idea that any spiral segment with a mathematical expression can be approximated by using this method. The main contribution of this thesis is this generalization. In Chapter 4, the analysis of deviation for each spiral is done according to *Theorem* 3.2 in Chapter 3. In Chapter 5, the implementation is shown by providing the pseudo-code of the program. In Chapter 6 some tables and figures present results of the approximation of some specific spiral segments. Finally Chapter 7 concludes the thesis with a general summary of the work accomplished, and points out some interesting results.

Chapter 2

Theoretical Background

In this chapter, the concept of a Pythagorean hodograph curve is explained and the merit of its algebraic characterization is mentioned. Pythagorean hodograph cubic and quintic Bézier are analyzed as examples. Biarc and its relevant property is introduced. We give definition and properties of quadratic Bézier, cubic Bézier, PH cubic, PH quintic Bézier, the clothoidal, the Archimedeans and the logarithmic spiral segments.

2.1 Pythagorean Hodograph Curves

Pythagorean hodograph curves were introduced to the CAD and CAGD community by Farouki and Sakkalis. In their paper [FS90], the definition and properties of Pythagorean hodograph curves are described clearly.

2.1.1 Introduction of Pythagorean Hodogragh

Parametric polynomial curves are an efficient and systematic form, and are widely used to represent curves and surfaces in CAD. For a plane curve segment, a polynomial curve can be defined as $\mathbf{Q}(t) = x(t)\mathbf{T}_0 + y(t)\mathbf{N}_0$ where x(t) and y(t) are polynomials in t, such as,

$$x(t) = \sum_{k=0}^{n} a_k t^k, \quad y(t) = \sum_{k=0}^{n} b_k t^k, \quad for \;\; t \in [0, 1]$$

and $\mathbf{T}_0$, $\mathbf{N}_0$ are the beginning unit tangent and normal vectors.

The computation of the polynomial curves is relatively easy for example the operations of addition and multiplication are easy. Polynomial curves form a subset of rational curves on which graphics packages are usually based. But a polynomial curve still has some significant shortcomings which hinder its overall usage in practical design application. If it is not a straight line, the points are usually not distributed uniformly along the curve when it is evaluated by evenly spaced parameter values t_k. To overcome this shortcoming, the functional relationship between the arc length along the curve and the parameter t is required. This function is an integral in general. Approximation of this integral may require a lot of computation and introduce errors. Another important deficiency is related to its "offset" curve. In applications, such as textile industry, shoe industry, car body industry and CNC machining, the curve $\mathbf{Q}_0(t) = \mathbf{Q}(t) + m\mathbf{n}(t)$ is widely used, i.e. $\mathbf{Q}_0(t)$ is a curve at m units away from a given curve $\mathbf{Q}(t)$ in the direction $\mathbf{n}(t)$, where $\mathbf{n}(t)$ is the unit normal of $\mathbf{Q}(t)$. In general if $\mathbf{Q}(t)$ is a polynomial curve, $\mathbf{Q}_0(t)$ is not a polynomial curve and not even a rational curve.

PH curves overcome these two disadvantages by virtue of the following properties:

- Their arclength is expressible in closed-form as polynomial functions.
- Their offsets are representable by rational curves of relatively low degree.

Since rational curves facilitate processings such as subdivision, transformation, intersection, etc., the second property gives PH curves an important role in geometric modeling systems.

2.1.2 Fundamentals of Pythagorean Hodographs

The following theorem is rephrased from [FS90]:

Theorem 2.1 Three real polynomials $a(t)$, $b(t)$ and $c(t)$, where the bigger degree between a and b is equal to the degree of c, satisfy the Pythagorean condition $a^2(t) + b^2(t) \equiv c^2(t)$ if and only if they can be expressed in terms of real polynomials $u(t)$, $v(t)$ and $w(t)$ in the form:

$$a(t) = w(t)[u^2(t) - v^2(t)],$$

$$b(t) = 2w(t)u(t)v(t),$$

$$c(t) = w(t)[u^2(t) + v^2(t)],$$

where $u(t)$ and $v(t)$ are relatively prime and $w(t)$ is the common factor of $a(t)$, $b(t)$ and $c(t)$.

In order to simplify computation, $w(t) = 1$ can be supposed in this thesis.

The following lemma is rephrased from [FS90]:

Lemma 2.1 Given a parametric curve $\mathbf{Q}(t) = x(t)\mathbf{T}_0 + y(t)\mathbf{N}_0$, the polynomial curve corresponding to the Pythagorean hodograph is given by setting

$$x'(t) = u^2(t) - v^2(t), \qquad y'(t) = 2u(t)v(t). \tag{2.1}$$

So that $\mathbf{Q}(t)$ is of degree $n = 2\mu + 1$, where $\mu = \max(\deg(u), \deg(v))$.

Notice that $n = 2\mu+1$ while deg(w)=0. To ensure that $\mathbf{Q}$(t) is indeed a PH curve. define $x'(t)$ and $y'(t)$ as $x'(t) = u^2(t) - v^2(t)$ and $y'(t) = 2u(t)v(t)$ as polynomials [FS90]. The curvature of a PH curve is [Far94]

$$\kappa(t) = \frac{2(u(t)v'(t) - u'(t)v(t))}{(u^2(t) + v^2(t))^2} \tag{2.2}$$

and the derivative of its curvature is [Far94]

$$\kappa' = \frac{2(uv'' - u''v)}{(u^2 + v^2)^2} - \frac{8(uv' - u'v)(uu' + vv')}{(u^2 + v^2)^3} \tag{2.3}$$

where the dependence on t is not shown for sake of readability.

2.1.3 Pythagorean Hodograph Cubic Bézier

A PH cubic, $\mathbf{Q}$(t), (also known as Tschirnhausen's cubic [FS90]) is the simplest Pythagorean hodograph curve of degree greater than 1. It has $n = 3$ and

$$w(t) = 1. \tag{2.4}$$

It can be obtained by defining $u(t)$ and $v(t)$ as

$$u(t) = u_0(1 - t) + u_1 t \tag{2.5}$$

and

$$v(t) = v_0(1 - t) + v_1 t$$

In this thesis it is assumed without loss of generality that $v_0 = 0$ for both the cubic and quintic PH curves [WM96b]. This forces $\mathbf{Q}'(0)$ to be parallel to $\mathbf{T}_0$. Hence,

$$v(t) = v_1 t. \tag{2.6}$$

Substitution of $w(t)$,$u(t)$ and $v(t)$ from Eqn. (2.4), (2.5) and (2.6) into Eqn. (2.1) gives:

$$\mathbf{Q}'(t) = x'(t)\mathbf{T}_0 + y'(t)\mathbf{N}_0 \tag{2.7}$$

where

$$x'(t) = u_0^2(1-t)^2 + 2u_0u_1(1-t)t + u_1^2t^2 - v_1^2t^2$$

and

$$y'(t) = 2u_0v_1t(1-t) + 2u_1v_1t^2.$$

An interesting geometric interpretation of the restrictions on the control polygon of a cubic Bézier curve to make the curve a PH cubic curve is the following. A PH curve is formed if and only if the following two conditions are met(see [FS90]):

$$L_2 = \sqrt{L_1L_3} \qquad \text{and} \qquad \theta_1 = \theta_2,$$

where L_1, L_2 and L_3 are the lengths of the control-polygon legs which are defined as $L_i = \| \mathbf{P}_i - \mathbf{P}_{i-1} \|$, and θ_1, θ_2 are the interior angles at vertices $\mathbf{P}_1$ and $\mathbf{P}_2$.

Another geometric property of PH cubics is that they have no real inflection points. The condition $\theta_1 = \theta_2$ makes the control polygon of a PH cubic convex so it is impossible to have an inflection point when $t \in [0, 1]$.

2.1.4 Pythagorean Hodograph Quintic Bézier

PH Cubics are not sufficiently flexible to interpolate discrete data sampled from a curvature continuous curve in which inflections are present. According to Farouki and Sakkalis [FS90], PH quintics can be categorized as cuspidal or non-cuspidal. The sign of the curvature changes at the inflection point in a cuspidal PH quintic.

In this thesis, only those PH quintic segments which are without cusps are discussed. According to [FS90], when the curvature of a PH quintic increase monotonically without changing sign, the control vertices form a convex shape.

A PH quintic Q(t) is obtained by defining $u(t)$ and $v(t)$ as [FS90]

$$u(t) = u_0(1-t)^2 + 2u_1(1-t)t + u_2t^2 \tag{2.8}$$

and

$$v(t) = v_0(1-t)^2 + 2v_1(1-t)t + v_2t^2$$

or with $v_0 = 0$, as is the convention in this thesis,

$$v(t) = 2v_1(1-t)t + v_2t^2 \tag{2.9}$$

From the formula we can tell that using PH quintics to fit a curvature continuous curve to discrete points is not as easy as with PH cubics.

2.2 Biarc

Let $\mathbf{A}_0$ and $\mathbf{A}_1$ be two successive data points that an interpolating curve is supposed to pass through, and let $\mathbf{T}_0$ and $\mathbf{T}_1$ be the tangential direction at these two points (as shown in Fig. (2.1)). The point $\mathbf{A}_2$ is the intersection of lines through $\mathbf{A}_0$ and $\mathbf{A}_1$ parallel to $\mathbf{T}_0$ and $\mathbf{T}_1$. $\mathbf{G}$ is somewhere in $\triangle\mathbf{A}_0\mathbf{A}_1\mathbf{A}_2$ where the two arcs join. From the conditions that the two arcs match the tangents $\mathbf{T}_0$ and $\mathbf{T}_1$ at $\mathbf{A}_0$ and $\mathbf{A}_1$ respectively and their tangents match at the joint, the location of $\mathbf{G}$ can not be determined uniquely. Let s be the length of the chord $\mathbf{A}_0\mathbf{A}_1$, $2a$ be the counter-clockwise angle from $\mathbf{A}_0\mathbf{A}_1$ to $\mathbf{A}_0\mathbf{A}_2$, $2b$ be the counter-clockwise angle from $\mathbf{A}_2\mathbf{A}_1$

to $\mathbf{A}_0\mathbf{A}_1$ and $2c$ be the counter-clockwise angle from $\mathbf{A}_0\mathbf{A}_1$ to the tangential direction at $\mathbf{G}$. The curvature of the two arcs can be expressed in terms of the angles $2a, 2b, 2c$ and the chord s which is equal to $\| \mathbf{A}_0\mathbf{A}_1 \|$ according to [Sab77] (p. 45).

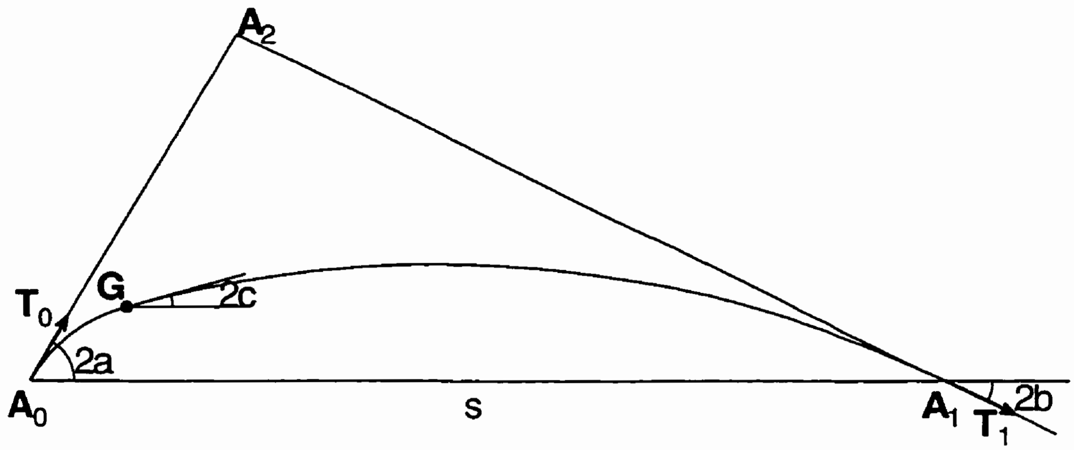

Figure 2.1: Biarc

the curvature of the first arc $\mathbf{A}_0\mathbf{G}$ is $-\frac{2\sin(b-a)\sin(a-c)}{s\sin(b+c)}$,

the curvature of the second arc $\mathbf{G}\mathbf{A}_1$ is $-\frac{2\sin(b-a)\sin(b-c)}{s\sin(a+c)}$.

Actually when $c = 0$, the tangent direction at point $\mathbf{G}$ is parallel to $\mathbf{A}_0\mathbf{A}_1$ and $\mathbf{G}$ is the incentre of the triangle $\mathbf{A}_0\mathbf{A}_1\mathbf{A}_2$.

2.3 Quadratic Bézier Spiral

Lemma 2.3 Given a beginning point, $\mathbf{P}_0$, beginning and ending unit tangent vectors, $\mathbf{T}_0$ and $\mathbf{T}_1$, respectively, Eqn (1.2) defines a quadratic Bézier segment when $n = 2$,

$$\mathbf{Q}(t) = \mathbf{P}_0(1-t)^2 + 2\mathbf{P}_1(1-t)t + \mathbf{P}_2 t^2. \tag{2.10}$$

where

$$\mathbf{P}_1 = \mathbf{P}_0 + a\mathbf{T}_0,$$

$$\mathbf{P}_2 = \mathbf{P}_1 + b\mathbf{T}_1, \tag{2.11}$$

for $a > 0$, $b > 0$, as illustrated in Fig. (2.2). Suppose θ is the counter-clockwise angle from $\mathbf{T}_0$ to $\mathbf{T}_1$ and let the ending curvature value, $c > 0$ be an extrema at $t = 1$. The Bézier segment is a spiral segment when

$$a = \frac{\tan\theta}{2c\cos\theta} \tag{2.12}$$

and

$$b = \frac{\tan\theta}{2c}. \tag{2.13}$$

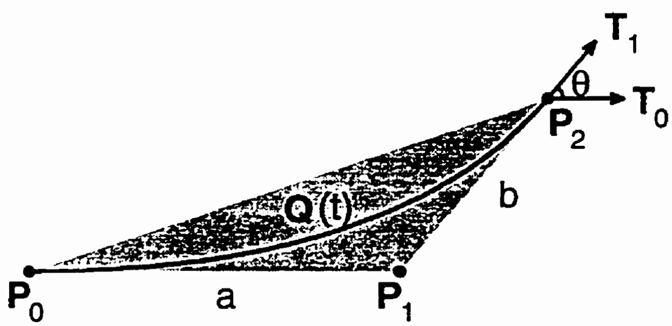

Figure 2.2: Quadratic Bézier Spiral Segment

Proof:

Denote $\mathbf{N}_0$ as the normal vector at $\mathbf{P}_0$. Substitute $\mathbf{P}_1$, $\mathbf{P}_2$ from Eqns.(2.11) into Eqn. (2.10) to obtain

$$\mathbf{Q}(t) = \mathbf{P}_0 + 2a\mathbf{T}_0 t + (b\mathbf{T}_1 - a\mathbf{T}_0)t^2 \tag{2.14}$$

Then take the derivative to obtain

$$\mathbf{Q}'(t) = 2(1-t)a\mathbf{T}_0 + 2bt\mathbf{T}_1 \tag{2.15}$$

and

$$\mathbf{Q}''(t) = -2a\mathbf{T}_0 + 2b\mathbf{T}_1 \tag{2.16}$$

So it follows that $\mathbf{Q}'''(t) = 0$. Since $\mathbf{T}_1 = (\cos\theta)\mathbf{T}_0 + (\sin\theta)\mathbf{N}_0$, Eqn.(2.15) and (2.16) can be rewritten as:

$$\mathbf{Q}'(t) = [2a(1-t) + 2bt\cos\theta]\mathbf{T}_0 + 2bt\sin\theta\mathbf{N}_0, \tag{2.17}$$

$$\mathbf{Q}'' = 2(b\cos\theta - a)\mathbf{T}_0 + 2b\sin\theta\mathbf{N}_0. \tag{2.18}$$

The signed curvature is defined by Eqn. (1.1).

$$\begin{aligned}\kappa(t) &= \frac{[2a(1-t)+2bt\cos\theta]2b\sin\theta + 2bt\sin\theta(2a-2b\cos\theta)}{(\sqrt{[2a(1-t)+2bt\cos\theta]^2 + (2bt\sin\theta)^2})^3} \\ &= \frac{4ab\sin\theta}{(\sqrt{4a^2(1-t)^2 + (8ab\cos\theta)t(1-t) + 4b^2t^2})^3}.\end{aligned} \tag{2.19}$$

The first derivative of (1.1), using $\mathbf{Q}'''(t) = 0$, yields

$$\kappa'(t) = \frac{-3\mathbf{Q}'(t)\times\mathbf{Q}''(t)}{(\mathbf{Q}'(t)\cdot\mathbf{Q}'(t))^{\frac{5}{2}}}\mathbf{Q}'(t)\cdot\mathbf{Q}''(t) \tag{2.20}$$

To force the curvature extremum to occur at the ending point, $\kappa'(1) = 0$ is required. Applying Eqns. (2.17), (2.18) to Eqn. (2.20) at $t = 1$, with $\kappa'(1) = 0$ leads to

$$b = a\mathbf{T}_0\cdot\mathbf{T}_1 = a\cos\theta. \tag{2.21}$$

The curvature at the ending is c, which means $\kappa(1) = c$. Using Eqn.(2.19) gives

$$\frac{4ab\sin\theta}{(2b)^3} = c$$

$$a = \frac{2b^2c}{\sin\theta} \tag{2.22}$$

From Eqn.(2.21) and (2.22), it follows that (2.12) holds. Eqn.(2.13) follows from (2.12) and (2.21). □

Using Eqn.(2.19), the curvature at $t = 0$ is equal to

$$\frac{4ab\sin\theta}{8a^3} = \frac{b\sin\theta}{2a^2}.$$

Applying Eqn.(2.21), it produces

$$\kappa(0) = \frac{\sin 2\theta}{4a}.$$

Since $a > 0$ and $a = \frac{\sin\theta}{2c\cos^2\theta}$, it follows that $\sin\theta > 0$, so $0 < \theta < \pi/2$ for a quadratic spiral segment.

This spiral segment has the following properties:

- Its curvature is equal to $\frac{\sin 2\theta}{4a}$ at $t = 0$.
- Its curvature is increasing monotonically.
- Its curvature has a local maximum at $t = 1$.

From Eqn.(2.10), it is known that a quadratic Bézier curve is a segment of a parabola. It has a curvature extremum at [WM94] :

$$t = \frac{a(a - b\cos\theta)}{a^2 + b^2 - 2ab\cos\theta}.$$

The curvature extremum is obtained by letting the first derivative of $\kappa'(t)$ equal to zero. In this case, Eqns.(2.16) and (2.18) are applied to Eqn.(2.20) and then $\kappa'(t) = 0$ gives the solution to the curvature extremum. Notice that if $t = 1$, it deduces Eqn.(2.21).

2.4 Cubic Bézier Spiral

Eqn(1.2) defines a cubic Bézier segment when $n = 3$.

$$\mathbf{Q}(t) = \mathbf{P}_0(1-t)^3 + 3\mathbf{P}_1(1-t)^2t + 3\mathbf{P}_2(1-t)t^2 + \mathbf{P}_3t^3. \tag{2.23}$$

where

$$
\begin{aligned}
\mathbf{P}_1 &= \mathbf{P}_0 + a\mathbf{T}_0, \\
\mathbf{P}_2 &= \mathbf{P}_1 + a\mathbf{T}_0, \\
\mathbf{P}_3 &= \mathbf{P}_2 + b\mathbf{T}_1.
\end{aligned} \tag{2.24}
$$

As shown in Fig. (2.3), $\mathbf{P}_0$, $\mathbf{P}_1$, $\mathbf{P}_2$, $\mathbf{P}_3$ form the control polygon of the spiral segment and $\mathbf{T}_0$, $\mathbf{T}_1$ are the unit tangent vectors at the beginning and ending points, respectively; $\mathbf{P}_0$, $\mathbf{P}_1$ and $\mathbf{P}_2$ are collinear and $\mathbf{P}_1$ is at the middle of the line segment $\mathbf{P}_1\mathbf{P}_2$. θ is the counter-clockwise angle from $\mathbf{P}_0\mathbf{P}_1$ to $\mathbf{P}_2\mathbf{P}_3$.

Suppose θ is the counter-clockwise angle from $\mathbf{P}_0\mathbf{P}_1$ to $\mathbf{P}_2\mathbf{P}_3$ and c is the ending curvature at $t = 1$, The cubic Bézier segment is a spiral segment when

$$a = \frac{25\tan\theta}{54c\cos\theta}$$

and

$$b = \frac{5\tan\theta}{9c}. \tag{2.25}$$

Eqns.(2.24) and (2.25) are derived in [WM96a].

The expressions of the function, first and second derivatives can be obtained from the above formulae. Substituting $\mathbf{Q}'(\mathbf{t})$ and $\mathbf{Q}''(\mathbf{t})$ in Eqn. (1.1),

$$\kappa(t) = \frac{216ct\cos^3\theta}{\{25 + 10t^2(6\cos^2\theta - 5) + t^4(25 - 24\cos^2\theta)\}^{\frac{3}{2}}} \tag{2.26}$$

As proved in [WM96a], this spiral segment has following properties:

- Its curvature is zero at $t = 0$.
- Its curvature has no extreme values and does not change sign for $0 < t < 1$.
- Its curvature has a local maximum at $t = 1$.

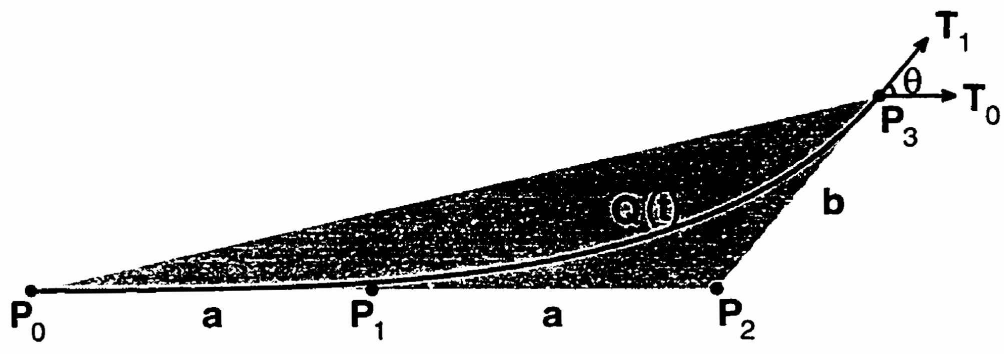

Figure 2.3: Regular Cubic Bézier Spiral Segment

2.5 PH Cubic Spiral

When $n = 3$, Eqn.(1.3) can be written as:

$$\mathbf{Q}'(t) = 3[(\mathbf{P}_1 - \mathbf{P}_0)t^2 + 2(\mathbf{P}_2 - \mathbf{P}_1)(1-t)t + (\mathbf{P}_3 - \mathbf{P}_2)(1-t)^2]$$

Comparing the coefficients of the terms $(1-t)^2, (1-t)t$ and t^2 to the corresponding ones in Eqn.(2.6) and (2.7), the relationships among the PH cubic vertices are obtained [FS90] as follows.

For $0 < \theta < \pi$, a PH cubic segment is given by

$$\begin{aligned}
\mathbf{P}_1 &= \mathbf{P}_0 + \frac{1}{3}u_0^2\mathbf{T}_0 \\
\mathbf{P}_2 &= \mathbf{P}_1 + \frac{1}{3}(u_0u_1\mathbf{T}_0 + u_0v_1\mathbf{N}_0) \\
\mathbf{P}_3 &= \mathbf{P}_2 + \frac{1}{3}[(u_1^2 - v_1^2)\mathbf{T}_0 + 2u_1v_1\mathbf{N}_0].
\end{aligned} \tag{2.27}$$

$\mathbf{T}_0$ and $\mathbf{T}_1$ are the unit tangent vector at the beginning and ending point respectively. Unit vector $\mathbf{N}_0$ is the normal vector at $\mathbf{P}_0$.

Given θ, the counter-clockwise angle from $\mathbf{T}_0$ to $\mathbf{T}_1$ and c, the extremum ending curvature at $t = 1$, the segment is a spiral segment if

$$u_0 = \sqrt{\frac{2\lambda(1+\lambda^2)}{c}} \tag{2.28}$$

$$u_1 = \frac{u_0}{1+\lambda^2} \tag{2.29}$$

and

$$v_1 = \lambda u_1. \tag{2.30}$$

where

$$\lambda = \frac{\sin\theta}{1+\cos\theta} > 0, \tag{2.31}$$

As illustrated in Fig. (2.4).

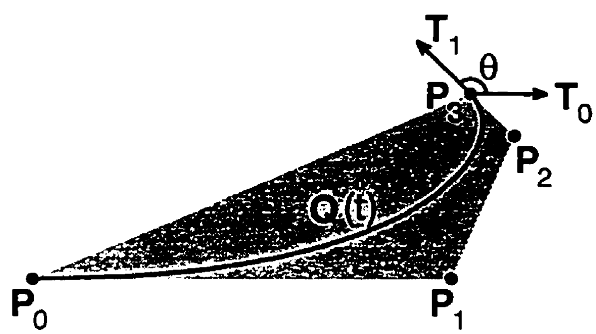

Figure 2.4: PH Cubic Spiral Segment

To verify Eqns.(2.28) to (2.30), observe that the relationships among $u_0, u_1$and v_1 are deduced by setting the initial conditions. Since $\mathbf{Q}'(0)$ is forced to be parallel to $\mathbf{T}_0$,

$$\tan\theta = \mathbf{Q}'(1).$$

Applying the condition $t = 1$ into Eqn.(2.6) and Eqn.(2.7), $\mathbf{Q}'(1)$ is given by:

$$\mathbf{Q}'(1) = (u_1^2 - v_1^2)\mathbf{T}_0 + 2u_1v_1\mathbf{N}_0.$$

These relationships are illustrated in Fig. (2.5). Expressions for $\sin\theta$ and $\cos\theta$ can be obtained from Fig. (2.5). Note that the restriction on θ causes $u_1 \neq 0$. Substitution

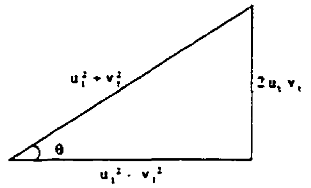

Figure 2.5: PH Cubic Tangent at $t = 1$

of the expressions for $\sin\theta$ and $\cos\theta$ into Eqn.(2.31) gives,

$$\lambda = \frac{\frac{2u_1v_1}{u_1^2+v_1^2}}{1+\frac{u_1^2-v_1^2}{u_1^2+v_1^2}} = \frac{v_1}{u_1}$$

So, Eqn.(2.30) holds. The first and second derivatives of Eqn.(2.4) and (2.5) are:

$$u'(t) = u_1 - u_0,$$

$$u''(t) = 0,$$

$$v'(t) = v_1 - v_0,$$

$$v'' = 0.$$

Replace $u'(t)$, $v'(t)$, $u''(t)$ and $v''(t)$ from above and $u(t)$, $v(t)$ from Eqn.(2.5) and (2.6) into Eqn.(2.2) and (2.3) to obtain,

$$\kappa(t) = \frac{2u_0v_1}{[u_0^2(1-t)^2 + 2u_0u_1(1-t)t + (u_1^2+v_1^2)t^2]^2} \tag{2.32}$$

$$\kappa'(t) = -\frac{8u_0v_1\{u_0(u_1-u_0) + [(u_1-u_0)^2+v_1^2]t\}}{[u_0^2(1-t)^2 + 2u_0u_1(1-t)t + (u_1^2+v_1^2)t^2]^3} \tag{2.33}$$

To make the ending curvature an extremum, the first derivative of the curvature at the ending point is set equal to zero. Therefore, $\kappa'(1) = 0$ which implies

$$u_0u_1 - u_0^2 + u_1^2 - 2u_0u_1 + u_0^2 + v_1^2 = 0$$

so,

$$u_1^2 + v_1^2 - u_0u_1 = 0$$

From Eqn.(2.30),

$$u_1^2(1+\lambda^2) - u_0 u_1 = 0$$

Hence,

$$u_1 = \frac{u_0}{1+\lambda^2}$$

which verifies Eqn.(2.29). Eqn.(2.28) can be obtained by substituting the given ending curvature c for the left hand side of Eqn.(2.32):

$$c = \kappa(1) = \frac{2u_0 v_1}{(u_1^2 + v_1^2)^2}$$

Using Eqn.(2.29) and Eqn.(2.30) to eliminate u_1 and v_1,

$$c = \frac{2u_0 \frac{\lambda u_0}{\lambda^2+1}}{\left\{(\frac{u_0}{1+\lambda^2})^2 + (\frac{\lambda u_0}{1+\lambda^2})^2\right\}^2} = \frac{2\lambda(1+\lambda^2)}{u_0^2}$$

So, Eqn.(2.28) holds.

When $t = 0$, $\kappa(t) = \frac{2v_1}{u_0{}^3}$. Applying Eqn.(2.24), (2.25) and (2.26) gives

$$\kappa(0) = \frac{c}{(1+\lambda^2)^2} \tag{2.34}$$

From Eqn.(2.33), since $\kappa'(t)$ only changes sign at one place, i.e. where $\kappa'(t) = 0$, it follows that $\kappa'(t) \neq 0$ in $[0, 1)$.

This spiral segments has the following properties:

- Its curvature is $\frac{c}{(1+\lambda^2)^2}$ at $t = 0$.
- Its curvature has no extreme values and does not change sign for $0 \leq t < 1$.

2.6 PH Quintic Spiral

According to [WM96b], a PH quintic spiral segment is given by

$$\mathbf{P}_1 = \mathbf{P}_0 + \frac{1}{5}u_0^2\mathbf{T}_0$$

$$\begin{aligned}
\mathbf{P}_2 &= \mathbf{P}_1 + \frac{1}{5}u_0^2\mathbf{T}_0 \\
\mathbf{P}_3 &= \mathbf{P}_2 + \frac{1}{15}(2u_0^2 + u_0u_2)\mathbf{T}_0 + \frac{1}{15}u_0v_2\mathbf{N}_0 \\
\mathbf{P}_4 &= \mathbf{P}_3 + \frac{1}{5}u_0u_2\mathbf{T}_0 + \frac{1}{5}u_0v_2\mathbf{N}_0 \\
\mathbf{P}_5 &= \mathbf{P}_4 + \frac{1}{5}(u_2^2 - v_2^2)\mathbf{T}_0 + \frac{2}{5}u_2v_2\mathbf{N}_0
\end{aligned} \tag{2.35}$$

where

$$\begin{aligned}
u_2 &= \frac{1}{2}\sqrt{\frac{7\sin\theta}{c}}, \\
u_0 &= \frac{49\lambda}{16cu_2}
\end{aligned} \tag{2.36}$$

and

$$v_2 = \lambda u_2,$$

where

$$\lambda = \frac{\sin\theta}{1+\cos\theta}.$$

for $0 < \theta < \pi$. The unit tangent vector at starting and ending point are $\mathbf{T}_0$ and $\mathbf{T}_1$, respectively. The unit normal vector of $\mathbf{T}_0$ is $\mathbf{N}_0$. θ is the counter-clockwise angle from $\mathbf{T}_0$ to $\mathbf{T}_1$, as shown in Fig. (2.6). Throughout this section it is assumed that the centre of the circle of curvature at $\mathbf{P}_5$ is to the left of the directed line through $\mathbf{P}_5$ in the direction of $\mathbf{T}_1$, i. e. , $c > 0$. The opposite case, i. e. $c < 0$, can be defined analogously.

It is shown in [WM96b] that the PH quintic Bézier defined in this way has the following properties.

- It is tangent to $\mathbf{T}_0$ and $\mathbf{T}_1$ at $t = 0$ and 1, respectively.
- It has zero curvature at $t = 0$.

- Its curvature has no extreme values and does not change sign for $0 < t < 1$.
- Its curvature has a local maximum at $t = 1$.

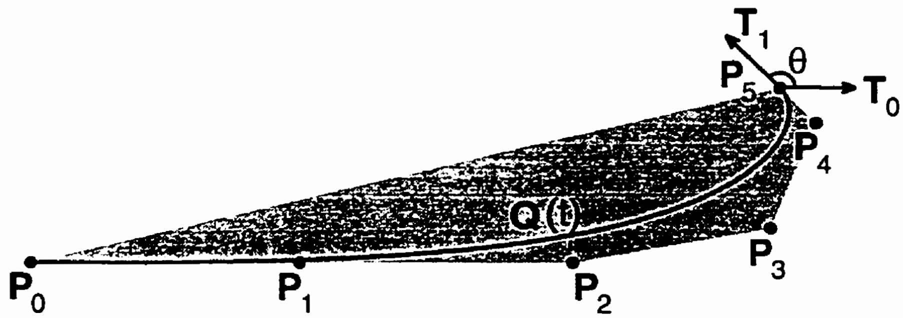

Figure 2.6: PH Quintic Spiral Segment

2.7 Clothoidal Spiral

2.7.1 Definition

The clothoid or Cornu spiral with scaling factor a is defined parametrically as

$$x(t) = aC(t), \quad y(t) = aS(t), \tag{2.37}$$

where C(t) and S(t) are the Fresnel integrals

$$C(t) = \int_0^t \cos(\pi\sigma^2/2)d\sigma$$

and

$$S(t) = \int_0^t \sin(\pi\sigma^2/2)d\sigma,$$

respectively, as shown in Fig. (2.7). The clothoid parameter t goes from negative infinity to positive infinity. It approaches the limiting point $(\frac{1}{2}a, \frac{1}{2}a)$ as t approaches infinity.

2.7.2 Properties

According to [MW89] some formulae for the clothoid are:

Angle of tangent:

$$\frac{1}{2}\pi t^2.$$

Curvature:

$$\kappa(t) = \pi t/a. \tag{2.38}$$

Arclength:

$$ds = adt. \tag{2.39}$$

Notice that an important property of the Cornu spiral is that its curvature varies linearly with its arclength.

The following equation shows the relationship among the constant a, the curvature, κ and the arclength s for clothoidal spirals. So if the arclength instead of the curvature of the ending point is known, the algorithm can still be applied. From Eqn.(2.37) and (2.38),

$$\kappa(t) = \frac{\pi t}{a} = \frac{\pi s}{a^2}.$$

So, if the arclength is s_e at $t = t_e$, where t_e is the ending point, and $c = \kappa(t_e)$,

$$c = \frac{\pi s_e}{a^2}$$

and

$$a = \frac{\pi t_e}{c},$$

so

$$t_e = \frac{s_e}{a}$$

which follows from Eqn.(2.38). Fig.(2.7) shows a clothoidal spiral with:

$a = 2, \quad t \in [-7, 7]$.

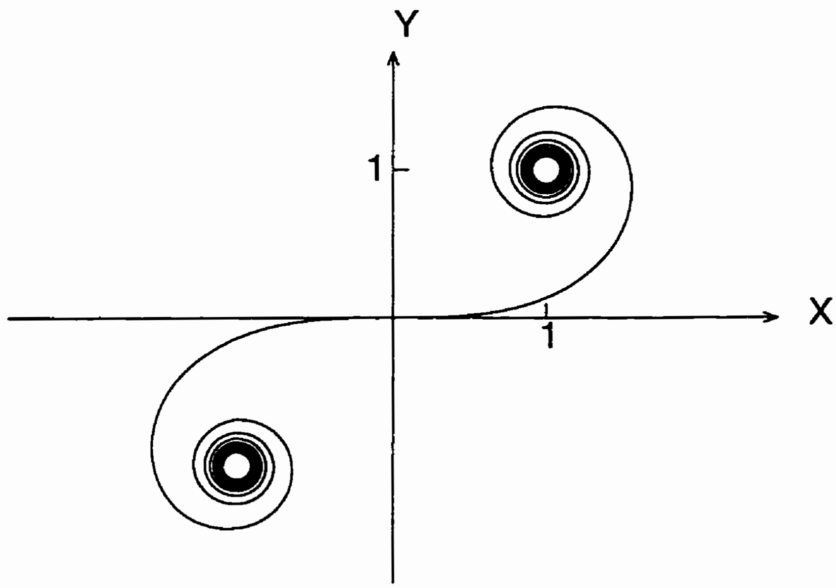

Figure 2.7: Clothoidal Spiral

2.7.3 Usage

The clothoid spiral is used for both highway and railway design. The clothoid transition can improve the stability of a vehicle when it traverses a curved roadway at a constant speed [Baa84].

The following are three types of road turnings. The comparison shows that using a clothoid as a transitional curve lessens sudden force and ensures the stability of the vehicle. In Fig.(2.8), Fig.(2.9) and Fig.(2.10), the following annotations are used. TS denotes point of change from tangent to spiral, SC denotes point of change from spiral to circular arc, CC denotes point of change from one circular arc to another. TC denotes point of change from tangent to circular arc and CT denotes point of

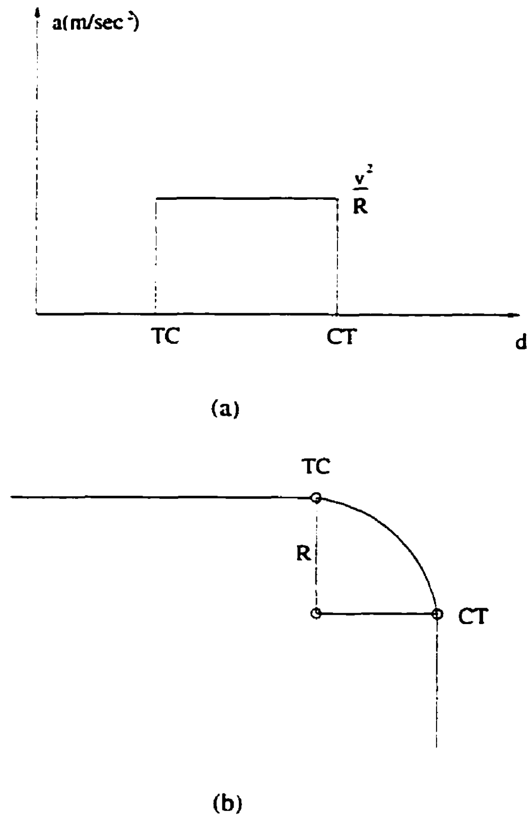

Figure 2.8: Circular Arc without Transition

change from circular arc to tangent. It is well known that a centripetal force is in direct proportion to the centripetal acceleration [Ada69] (p. 149), a, where

$$a = \frac{v^2}{r}.$$

Therefore, the more r changes gradually, the less the sudden force is. In another words, a continuous instead of abrupt change of the curvature is expected to avoid the sudden force.

(i) As shown in Fig.(2.8), a vehicle encounters a sudden change in centripedal acceleration when it moves from a straight line to a circular arc or moves from a circular arc to a straight way. Part a shows acceleration changes from 0 to $\frac{v^2}{R}$

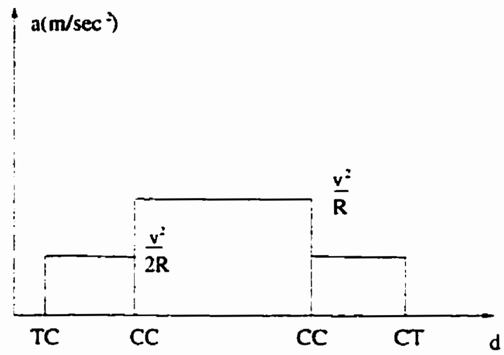

(a)

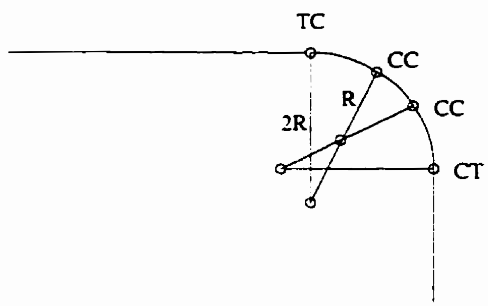

(b)

Figure 2.9: Compound Circular Arc

and from $\frac{v^2}{R}$ to 0 at point TC and CT, respectively. Part b is the route of the vehicle.

(ii) When the road turning is composed of several circular arcs (as illustrated in Fig. (2.9)), the centripedal acceleration increases and decreases like a staircase. In part a, the acceleration changes as such $0 \rightarrow \frac{v^2}{2R} \rightarrow \frac{v^2}{R} \rightarrow \frac{v^2}{2R} \rightarrow 0$, at TC, CC, CC and CT, respectively. Part b shows the route of the vehicle and the radius of the arcs at those points. It is a better than the first case, because the discontinuity forces on those points are less than the ones in the first case.

(iii) The ideal design is to have continuously increasing or decreasing centripedal

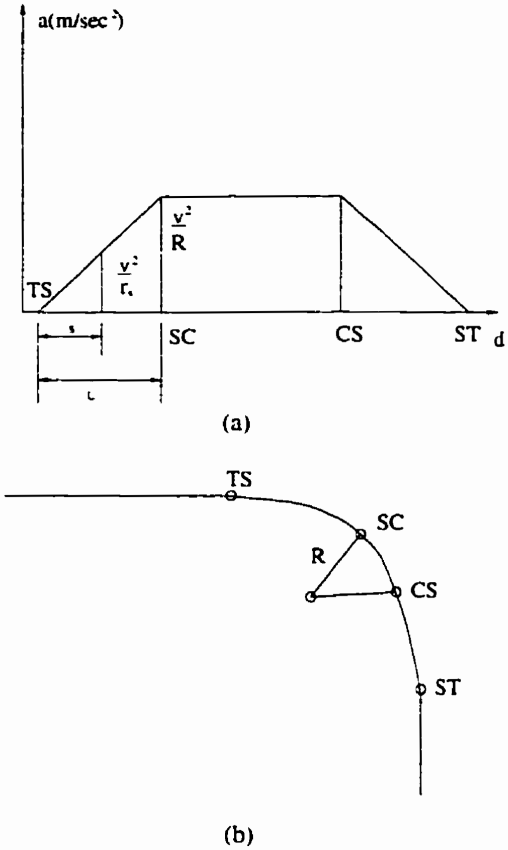

Figure 2.10: Circular Arc with Spiral Transition

acceleration, as shown in Fig.(2.10). In Part a, the centripedal acceleration changes continuously from 0 to $\frac{v^2}{R}$ in the interval $[TS, SC]$, and it changes from $\frac{v^2}{R}$ to 0 in the interval $[CS, ST]$. Part b shows the joint of tangent lines, transition curves and the circular arc.

The following is the analysis of case(iii) in the interval $[TS, SC]$.

In this case the acceleration rate is a linear function of its arc length. Referring to Fig.(2.11), denote s as the arclength of the curve when the tangent direction changes as much as θ counter-clockwise from TS, r as its corresponding radius and L as the

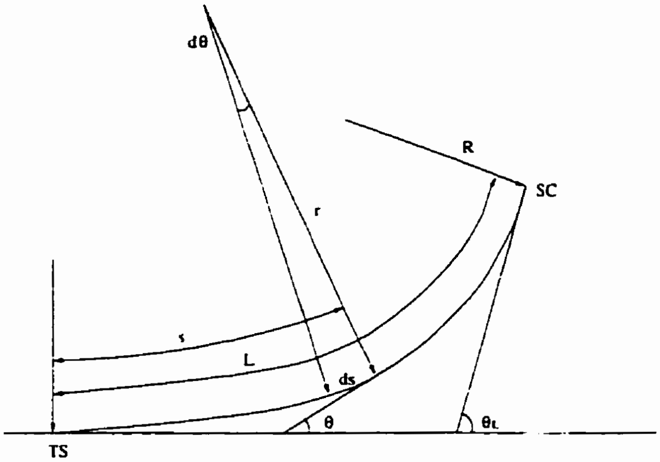

Figure 2.11: Transition Curve

total length of the curve from TS to SC. Therefore,

$$\frac{\frac{v^2}{r}}{\frac{v^2}{R}} = \frac{s}{L},$$

eliminating v yields

$$rs = RL.$$

R and L are constant in a given condition. Suppose $RL = A^2$, where A is a constant, then

$$rs = A^2, \tag{2.40}$$

When ds, the differential sector, is infinitesimally small, it follows for the osculating circle that

$$d\theta = \frac{ds}{r},$$

as shown in Fig.(2.11). Notice that $\frac{d\theta}{ds}$ can also be taken as the definition of curvature κ. Substitution of r from Eqn.(2.40) gives

$$d\theta = \frac{1}{A^2} s ds.$$

After integrating, it becomes

$$s = A\sqrt{2\theta}. \tag{2.41}$$

When ds is infinitesimally small,

$$dx = \cos\theta ds$$

$$dy = \sin\theta ds. \tag{2.42}$$

Substitution of s from Eqn.(2.41) and integration of the above two equations gives:

$$x = \frac{A}{\sqrt{2}}\int_0^\theta \frac{\cos\theta}{\sqrt{\theta}}d\theta$$

$$y = \frac{A}{\sqrt{2}}\int_0^\theta \frac{\sin\theta}{\sqrt{\theta}}d\theta. \tag{2.43}$$

Replacing the variable θ with $\frac{\pi\sigma^2}{2}$ produces

$$x = \frac{A}{\sqrt{2}}\int_0^{\sqrt{\frac{2\theta}{\pi}}} \frac{\cos(\frac{\pi}{2}\sigma^2)}{\sqrt{\frac{\pi}{2}}\sigma}d(\frac{\pi}{2}\sigma^2) = A\sqrt{\pi}\int_0^{\sqrt{\frac{2\theta}{\pi}}} \cos(\pi\sigma^2/2)d\sigma. \tag{2.44}$$

Similarly,

$$y = A\sqrt{\pi}\int_0^{\sqrt{\frac{2\theta}{\pi}}} \sin(\pi\sigma^2/2)d\sigma. \tag{2.45}$$

Comparing Eqn.(2.42) and (2.43) with Eqn.(2.37), the transition curve is actually the clothoid with

$$a = \sqrt{\pi}A, \qquad t = \sqrt{\frac{2\theta}{\pi}}. \tag{2.46}$$

To join a circle and a line, a clothoid can be uniquely determined. The scale factor can be calculated by letting the curvature of the spiral equal to the reciprocal of the radius of the circle. To join two circles with a compound S curve (reverse curve) matching the curvature somewhere around two separate circles, two reverse clothoids that meet with zero curvature can be found. To join two circles with a compound C curve(broken-back curve), two clothoids can be found [MW89]. To facilitate the drawing of the clothoid arc, templates with scales are commonly used [Baa84].

2.7.4 Highway Spiral and the Clothoid

The highway spiral is defined in [Hic67]. It is actually the same spiral as mentioned in the last section. Using the same notation as in section (2.7.3), the formula in [Hic67] (p. 171) is

$$\theta = \frac{s^2}{2RL}, \tag{2.47}$$

As we know,

$$d\theta = \frac{s ds}{A^2}. \tag{2.48}$$

After taking the integral of both sides, it becomes

$$\theta = \frac{s^2}{2A^2} \tag{2.49}$$

Using the assumption $RL = A^2$, Eqn.(2.47) follows.

Observe the first derivative of the two spirals:

For a clothoidal spiral, because $\frac{ds}{dt} = a$ from Eqn.(2.39) and $(\frac{dx}{dt}, \frac{dy}{dt}) = (a \cos \frac{\pi t^2}{2}, a \sin \frac{\pi t^2}{2})$, hence

$$\frac{ds}{dx} = \frac{ds}{dt} * \frac{dt}{dx} = \frac{1}{\cos(\frac{\pi}{2}t^2)},$$

$$\frac{ds}{dy} = \frac{ds}{dt} * \frac{dt}{dy} = \frac{1}{\sin(\frac{\pi}{2}t^2)},$$

where $\frac{\pi}{2}t^2$ is the angle of tangent at point t. For a highway spiral defined by [Hic67] or from Eqns.(2.42),

$$\frac{ds}{dx} = \frac{1}{\cos\theta}, \tag{2.50}$$

$$\frac{ds}{dy} = \frac{1}{\sin\theta}, \tag{2.51}$$

where θ is the angle of tangent. From Eqn.(2.46), $\theta = \frac{\pi}{2}t^2$ which means the first derivative or the hodograph of the highway spiral and the clothoid is actually the same.

So the angle of tangent of highway spiral is $\frac{1}{2}\pi t^2$ which is equal to $\frac{1}{2}\pi\frac{s^2}{a^2}$. Comparing θ in highway spiral and the angle of tangent defined in the clothoid,

$$\frac{1}{2}\pi\frac{s^2}{a^2} = \frac{s^2}{2RL},$$

Hence,

$$a = \sqrt{\pi RL},$$

where $L = 2R\theta_L$. This equation gives us a one to one relationship between the initial parameters of the clothoid and the highway spiral.

Before widespread accessibility of computers, it was very cumbersome to calculate Fresnel integrals. People used to simplify the computation of the highway spiral by using power series with high order terms omitted. Hickerson presents an approximation for the highway spiral as follows.

After expanding the sine function and integrating Eqn.(2.37), it follows that:

$$y = \frac{s}{100}[0.58\theta - \cdots].$$

Application of Eqn.(2.47) gives an approximation using only the first term.

$$y = \frac{s^3}{6RL}.$$

It shows that the highway spiral is very similar to a cubic polynomial.

2.8 Archimedean Spiral

Referring to [vS90] (p.124) an Archimedean spiral is defined as

$$r = a\theta^{\frac{1}{m}}$$

or

$$(x^2 + y^2)^{\frac{m}{2}} - a^m arctan(y/x) = 0$$

where a and m are constants.

It can also be defined parametrically as

$$x(t) = at^{\frac{1}{m}} \cos t$$

$$y(t) = at^{\frac{1}{m}} \sin t \tag{2.52}$$

An Archimedean spiral with $a = 0.35$, $m = 2$ and $t \in [0.01, 20]$ is shown in Fig.(2.12).

2.9 Logarithmic Spiral

2.9.1 Definition and Equiangular Property

Referring to [BF97] a logarithmic spiral is defined as

$$r = r_0 e^{k\theta} \tag{2.53}$$

or

$$\ln[(x^2 + y^2)/r_0^2]/2 - k \cdot \arctan(y/x) = 0$$

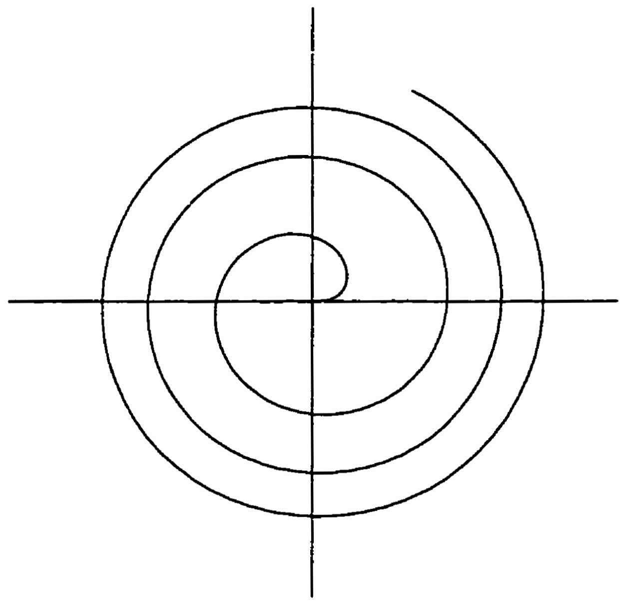

Figure 2.12: Archimedean spiral with $m = 2$

where k is a constant and r_0 is the beginning radius of curvature (a constant). It can also be defined parametrically as

$$x(t) = r_0 e^{kt} \cos t$$

$$y(t) = r_0 e^{kt} \sin t \tag{2.54}$$

respectively. Fig.(2.13) shows a logarithmic spiral with:

$r_0 = 0.1, \quad k = 0.15 \quad t \in [0, 20]$.

Consider a ray drawn from the origin to a point (x, y) on the logarithmic spiral. Let ϕ be the angle made by the ray and the unit tangent to the spiral at (x, y). Now

$$\cos\phi = \frac{(x,y)}{\| (x,y) \|} \cdot \frac{(x',y')}{\| (x',y') \|}. \tag{2.55}$$

The first derivative of the parameter form of the logarithmic spiral is

$$x'(t) = r_0 k e^{kt} \cos t - r_0 e^{kt} \sin t,$$

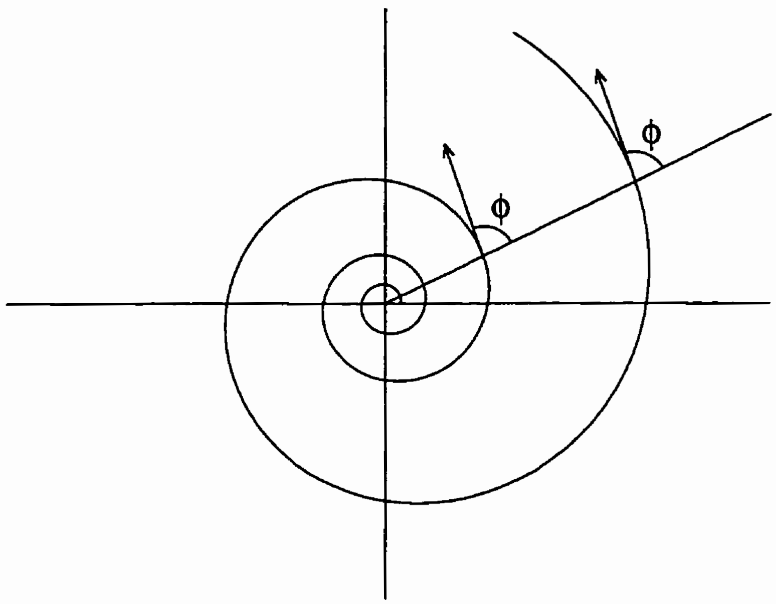

Figure 2.13: Logarithmic Spiral

$$y'(t) = r_0 k e^{kt} \sin t + r_0 e^{kt} \cos t. \tag{2.56}$$

So,

$$\begin{aligned}
\| (x', y') \|^2 &= r_0^2 k^2 e^{2kt} \cos^2 t + r_0^2 e^{2kt} \sin^2 t - 2 r_0^2 k e^{2kt} \sin t \cos t \\
&\quad + r_0^2 k^2 e^{2kt} \sin^2 t + r_0^2 e^{2kt} \cos^2 t + 2 r_0^2 k e^{2kt} \sin t \cos t \\
&= r_0^2 e^{2kt} (k^2 + 1)
\end{aligned}$$

$$\| (x', y') \| = r_0 e^{kt} \sqrt{k^2 + 1} \tag{2.57}$$

Use of Eqn.(2.54), (2.56) and (2.57) in (2.55) yields

$$\begin{aligned}
\cos \phi &= \frac{r_0^2 k e^{2kt} \cos^2 t - r_0^2 e^{2kt} \sin t \cos t + r_0^2 k e^{2kt} \sin^2 t + r_0^2 e^{2kt} \sin t \cos t}{r_0^2 e^{2kt} \sqrt{k^2 + 1}} \\
&= \frac{k}{\sqrt{k^2 + 1}}
\end{aligned}$$

Since k is a constant, it thus follows that the angle made by the unit tangent and the ray is a constant at the intersection of the ray and the logarithmic spiral. So, the logarithmic spiral is also called the equiangular spiral.

2.9.2 Transformation

Suppose $\mathbf{i}, \mathbf{j}$ are the unit vectors of direction $x(t)$ and $y(t)$ respectively, then

$$\mathbf{Q}(t) = x(t)\mathbf{i} + y(t)\mathbf{j}$$

and

$$\begin{aligned}\mathbf{Q}'(t) &= r_0 e^{kt}(k\mathbf{i}+\mathbf{j})\cos t + r_0 e^{kt}(k\mathbf{j}-\mathbf{i})\sin t. \\ &= r_0\sqrt{k^2+1}e^{kt}\{\frac{k\mathbf{i}+\mathbf{j}}{\sqrt{k^2+1}}\cos t + \frac{k\mathbf{j}-\mathbf{i}}{\sqrt{k^2+1}}\sin t\}\end{aligned}$$

Observe that $\frac{k\mathbf{i}+\mathbf{j}}{\sqrt{k^2+1}}$ and $\frac{k\mathbf{j}-\mathbf{i}}{\sqrt{k^2+1}}$ form an orthogonal pair, and that

$$\mathbf{Q}'(0) = r_0(k\mathbf{i}+\mathbf{j}),$$

i.e. $\frac{k\mathbf{i}+\mathbf{j}}{\sqrt{k^2+1}}$ and $\frac{k\mathbf{j}-\mathbf{i}}{\sqrt{k^2+1}}$ are the beginning unit tangent and normal vectors respectively of the logarithmic spiral. Denote them respectively as $\mathbf{T}_0$ and $\mathbf{N}_0$, replace r_0 by $\frac{1}{c_0}$ and scale the spiral so that

$$\mathbf{Q}'(t) = \frac{e^{kt}}{c_0}(\cos t\mathbf{T}_0 + \sin t\mathbf{N}_0), \quad 0 \le t \le \theta. \tag{2.58}$$

Integration of Eqn.(2.58) gives

$$\begin{aligned}\mathbf{Q}(t) &= \mathbf{P}_0 + \frac{1}{c_0(k^2+1)}\{[e^{kt}(k\cos t + \sin t) - k]\mathbf{T}_0 \\ &\quad +[e^{kt}(k\sin t - \cos t) + 1]\mathbf{N}_0\}, \quad 0 \le t \le \theta.\end{aligned} \tag{2.59}$$

From Eqn.(2.58), $\| \mathbf{Q}'(t) \| = \frac{e^{kt}}{c_0}$, and

$$\mathbf{Q}''(t) = \frac{e^{kt}}{c_0}[(k\cos t - \sin t)\mathbf{T}_0 + (k\sin t + \cos t)\mathbf{N}_0], \tag{2.60}$$

so

$$\begin{aligned}\mathbf{Q}'(t) \times \mathbf{Q}''(t) &= \frac{e^{2kt}}{c_0^2}(k\cos t\sin t + \cos^2 t - k\cos t\sin t + \sin^2 t) \\ &= \frac{e^{2kt}}{c_0^2}\end{aligned}$$

Substitute the results into Eqn.(1.1) to obtain

$$\kappa(t) = \frac{c_0}{e^{kt}} \quad > 0.$$

Observe that the curvature at the beginning is c_0 when $t = 0$. Let the ending curvature be c when $t = \theta$, hence,

$$c = \frac{c_0}{e^{k\theta}},$$

$$e^{k\theta} = \frac{c_0}{c},$$

so

$$k = \frac{1}{\theta}\ln(\frac{c_0}{c}). \tag{2.61}$$

2.9.3 Relationship between Logarithmic Spiral and Archimedean Spiral

The following is stated in [Yat52] (p. 211).

> *The orthographic projection of a Conical Helix on a plane perpendicular to its axis is a Spiral of Archimedes. The development of this Helix, however, is an Equiangular spiral.*

This statement is illustrated in Fig.(2.14). It shows a conical Helix $(a(1-\frac{\theta}{2\pi})\cos\theta, a(1-\frac{\theta}{2\pi})\sin\theta, \frac{\theta}{2\pi}b)$ with a=0.8 b=1.8. "A" denotes the Archimedean spiral, "L" denotes logarithmic spiral and "C" denotes the base of the cone. The Archimedean spiral is obtained by ignoring the variance in the h direction. The function of it is $(a(1-\frac{\theta}{2\pi})\cos\theta, a(1-\frac{\theta}{2\pi})\sin\theta)$. When the surface of the cone is opened along the edge where $\theta = 0$, the curve in the fan thus formed is a logarithmic spiral. The angle of the fan is $\frac{2\pi r}{\sqrt{r^2+h^2}}$ since the circle of the base is equal to the arclength of the fan. The points evenly lying on $\theta \in [0, 2\pi]$ are distributed evenly in the interval $[0, \frac{2\pi r}{\sqrt{r^2+h^2}}]$ and the points can be located according to its distance to the top of the cone.

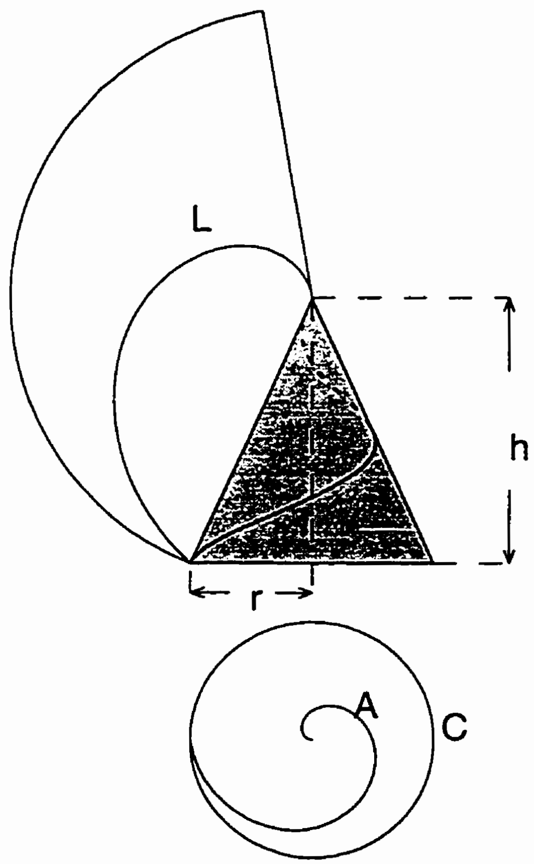

Figure 2.14: Logarithmic and Archimedean Spiral

2.9.4 Applications of Logarithmic Spiral and Archimedean Spiral

The logarithmic spiral occurs often in nature. Some creatures build logarithmic spirals during their growths, such as the septa of the Nautilus, the arrangement of seeds in the sunflower and the formation of pine cones.

The loxodromic spiral, also called loxodrome [Mor92](p. 1351), is any curve on a given surface of revolution that intersects each meridians of the curve at some constant angle which is not equal to ninety degrees. For example, when a train moves toward a fixed direction, it intersects the meridian at some constant angle. the projection of its route on the equator plane is an equiangular spiral.

The Archimedean spiral with parameter $m = 1$ is used as a cam to produce linear motion. The cam is pivoted at the pole and rotated with constant angular velocity. The piston, kept in contact with a spring device, has uniform reciprocating motion.

Chapter 3

Generalization

3.1 Generalized Theorem

From the approximation of quadratic and cubic spirals, a general way may be found to approximate other spirals. The algorithm used to generate the curve of the approximation problem is based on the theorems outlined below. In this chapter. two theorems are presented to generalize the approximation of any spiral. The basic idea of this approximation is to construct a control triangle determined by the starting point, the ending point and their tangent directions. A biarc, whose joint is at the incentre of the triangle, can be fitted through the starting and the ending points such that it is tangent to the triangle at these two points. *Theorem* 3.1 gives the radial deviation of the spiral from the joint of the biarc. Since the maximum deviation is highly dependent on the individual spiral, *Theorem* 3.2 gives a general result of where local extrema in the deviation of a spiral from an approximating biarc may occur. From that the maximum deviation can be determined.

The following lemma is used in *Theorem* 3.1.

Lemma 3.1 Given a winding spiral segment whose tangent rotates by less than π. It starts from $\mathbf{P}_0$, with non-zero curvature and unit tangent vector $\mathbf{T}_0$, and ends at $\mathbf{P}_2$ with unit tangent vector $\mathbf{T}_1$. Then $0 < \theta < \pi$, where θ is the angle from $\mathbf{T}_0$ to $\mathbf{T}_1$, the angle from $\mathbf{T}_0$ to the line segment joining $\mathbf{P}_0$ to $\mathbf{P}_2$ is less than $\pi/2$.

Proof:

Denote $\angle\mathbf{P}_2\mathbf{P}_0\mathbf{P}_1$ as α, $\angle\mathbf{P}_0\mathbf{P}_2\mathbf{P}_1$ as β, as shown in Fig. (3.1). Vogt's theorem [Gug63](p. 49) says α is smaller than β in a winding spiral. Since θ is the sum of those two angles, α is less than $\frac{\theta}{2}$. Now $0 < \theta < \pi$, so

$$0 < \alpha < \frac{\theta}{2} < \frac{\pi}{2}.\Box$$

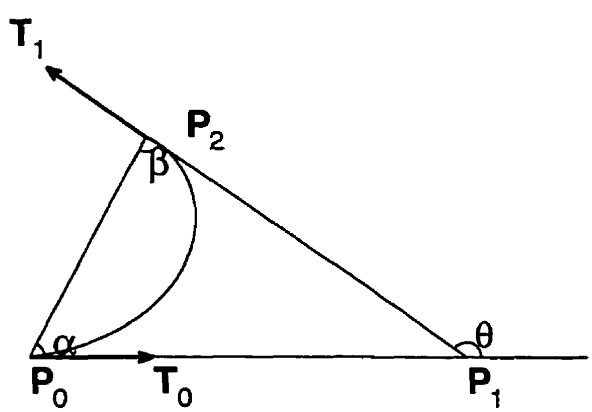

Figure 3.1: Spiral Triangle

The theorems that will be used for applying a biarc approximation are now presented.

Theorem 3.1 Given a spiral segment $\mathbf{Q}(t), t_0 < t < t_1$, with beginning and ending points $\mathbf{A}_0 = \mathbf{Q}(t_0)$ and $\mathbf{A}_1 = \mathbf{Q}(t_1)$, respectively. Let $\mathbf{V}$ be the intersection

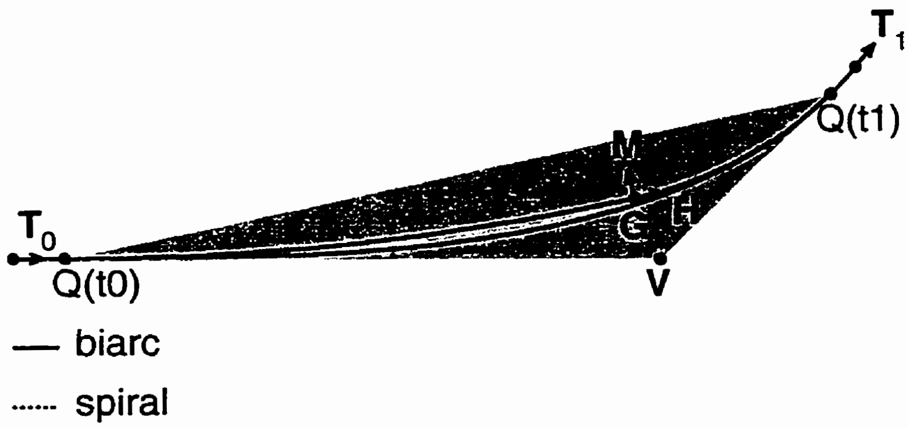

Figure 3.2: Biarc Approximation of Spiral Segment

of the straight lines parallel to $\mathbf{Q}'(t_0)$ and $\mathbf{Q}'(t_1)$ through $\mathbf{A}_0$ and $\mathbf{A}_1$ respectively, as illustrated in Fig. (3.2). Let the triangle $\mathbf{A}_0$,$\mathbf{V}$ and $\mathbf{A}_1$ define a biarc where the two arcs are $\mathbf{G}^1$ continuous at the joint which is the incentre of the triangle. Let $\mathbf{H}$ and $\mathbf{M}$ be the unit tangent and normal vectors, respectively, of the biarc at its joint, $\mathbf{G}$. The deviation of the spiral from the joint of the biarc, measured along the radial direction of the biarc is given by

$$d = \{\mathbf{Q}(\eta) - \mathbf{G}\} \cdot \mathbf{M}$$

where η is the unique value that satisfies

$$\{\mathbf{Q}(\eta) - \mathbf{G}\} \cdot \mathbf{H} = 0, \quad t_0 < \eta < t_1. \tag{3.1}$$

Proof.

It suffices to find d and η that satisfy

$$\mathbf{G} + d\mathbf{M} = \mathbf{Q}(\eta), \quad t_0 < \eta < t_1,$$

or

$$\mathbf{Q}(\eta) - \mathbf{G} = d\mathbf{M}, \quad t_0 < \eta < t_1 \tag{3.2}$$

Taking the dot product of (3.2) with $\mathbf{H}$ yields

$$f(\eta) = \{\mathbf{Q}(\eta) - \mathbf{G}\} \cdot \mathbf{H} = 0. \tag{3.3}$$

Since $\mathbf{G}$ is the incentre of the triangle with vertices $\mathbf{Q}(t_0)$, $\mathbf{V}$ and $\mathbf{Q}(t_1)$ it follows that $\mathbf{H}$ is approximately parallel to, and has the same orientation as the directed line segment $\mathbf{Q}(t_0)\mathbf{Q}(t_1)$ (Refer to [Sab77] p. 45). Also by *Lemma* 3.1, the angle from $\mathbf{Q}(t_0) - \mathbf{G}$ to $\mathbf{H}$ is larger than $\pi/2$ and less than π; the angle from $\mathbf{Q}(t_1) - \mathbf{G}$ to $\mathbf{H}$ is less than $\pi/2$ and larger than zero. Hence,

$$f(t_0) = \{\mathbf{Q}(t_0) - \mathbf{G}\} \cdot \mathbf{H} < 0$$

and

$$f(t_1) = \{\mathbf{Q}(t_1) - \mathbf{G}\} \cdot \mathbf{H} > 0$$

The direction of $\mathbf{Q}'(\eta)$ varies monotonically from the direction $\mathbf{T}_0$ to $\mathbf{T}_1$. Any ray from a point on the line segment $\mathbf{Q}(t_0)\mathbf{Q}(t_1)$ can intersect the spiral segment at most once. Therefore, the line through $\mathbf{G}$ parallel to $\mathbf{M}$ intersects the spiral only once at unique $t = \eta$. Hence, the theorem follows. □

The Newton-Raphson method should work well in solving Eqn. (3.1) because $f(\eta)$ is monotone for $t_0 \leq \eta \leq t_1$, but if it does not, the bisection method will always work. Note that numerical root-finding methods are not necessary for the quadratic spiral segment.

Theorem 3.2 Given a spiral segment, $\mathbf{Q}(\mathrm{t})$ as defined for *Theorem* 3.1. Let $\mathbf{A}_0 = \mathbf{Q}(t_0)$, $\mathbf{A}_1 = \mathbf{Q}(t_1)$, and $\mathbf{V}$ be as for *Theorem* 3.1. Let the triangle $\mathbf{A}_0$,$\mathbf{V}$ and $\mathbf{A}_1$ define a biarc where the two arcs are $\mathbf{G}^1$ continuous at the joint, which is the incentre of the triangle. Let $\mathbf{C}_i$ and r_i be the centre and radius, respectively, of that arc of the biarc that passes through $\mathbf{Q}(t_i)$ and let $\mathbf{H}_i$ and $\mathbf{M}_i$ be the unit tangent and normal vectors, respectively, of the biarc at $\mathbf{Q}(t_i)$. Let η be as determined by *Theorem* 3.1. The deviation of the spiral from the biarc, measured along a radial direction of the biarc, has at most one local extremum for $t_0 < t \leq \eta$ and at most one local extremum for $\eta < t \leq t_1$. These local extrema, if one or more of them exist, occur at values of t that satisfy

$$g_i(t) = \{\mathbf{Q}(t) - \mathbf{C}_i\} \cdot \mathbf{Q}'(t) = 0. \tag{3.4}$$

Proof.

It follows from the definition of the biarc that

$$\mathbf{C}_i = \mathbf{Q}(t_i) + r_i\mathbf{M}_i, \quad i = 0, 1.$$

The deviation $|h_i(t) - r_i|$ has an extremum at the same place as the square of the deviation. It is required to show that the square of the radial deviation,

$$e_i(t) = \{h_i(t) - r_i\}^2,$$

has at most one local maximum for each of $i = 0$ and $i = 1$. Define

$$h_i(t) = \| \mathbf{Q}(t) - \mathbf{C}_i \|,$$

so $h_i(t) > 0$ and

$$h_i^2(t) = \{\mathbf{Q}(t) - \mathbf{C}_i\} \cdot \{\mathbf{Q}(t) - \mathbf{C}_i\} > 0. \tag{3.5}$$

Now $e_i'(t) = 2\{h_i(t) - r_i\}h_i'(t)$, and $e'(t)$ will be zero at both maximal and minimal values of $e_i(t)$. $e_i'(t) = 0$ when $h_i(t) - r_i = 0$ or $h_i'(t) = 0$. $e_i(t)$ is minimized for $h_i(t) - r_i = 0$; hence, the necessary condition for $e_i(t)$ to have a local maximum is $h_i'(t) = 0$. From Eqn.(3.4), assuming $h_i(t) \neq 0$, this condition is equivalent to Eqn.(3.3).

The arc centered at $\mathbf{C}_i$ has a point of contact (i. e. matching in position and tangential direction) with the spiral at $t = t_i$. A result of Vogt[[Gug63], p. 53], states that a circle and a convex spiral can have at most three points of intersection, or one point of contact and one non-contact intersection. It thus follows that between the point of contact and the point of intersection the tangential direction of $\mathbf{Q}(t)$ at some point, t_p is parallel to the tangential direction of the circle centred at $\mathbf{C}_i$ at which the circle and the normal vector at t_p intersect. Hence, the arc centred at $\mathbf{C}_i$ can have at most one point other than $\mathbf{Q}(t_i)$ for which (3.3) is satisfied and for which t lies between t_i and η.

Hence the theorem follows. □

When comparing these results to the optimal method of [MP84], observe that the biarc approximation matches the beginning and ending points and tangential directions of the spiral segment which make the tangential directions continuous at the joints when a spiral is approximated segment by segment. The given tangential directions and positions of the spiral at the beginning are not matched when using the method in [MP84]. That method works well when a spiral is approximated by one whole piece because of fewest piecewise arcs and the maximum deviation is reached according to the algorithm. However, this approximation might cause sudden changes in the position and direction of the machine tool at points on the object where the design involves two spiral segments intended to be joined smoothly. Furthermore, the method of [MP84] is based on nonlinear optimization which could be computationally complex and may not be straightforward to implement.

3.2 Location of Local Maxima

3.2.1 Polynomial Spiral Segment

For a specific i, Eqn(3.3) is in general a nonlinear equation with at most two solutions including the one at $t = t_i$. When applying numerical root-finding methods, it is desirable that the equation have a unique solution to avoid convergence to the wrong solution. When $\mathbf{Q}(t)$ is a parametric polynomial spiral segment, Eqn. (3.3) is polynomial in which case the solution at $t = t_i$ can be factored out resulting in a polynomial equation of lower degree and with at most one solution. In this case the bisection method can be used to check if a solution does exist. If a solution exists, the bisection method can be used in combination with the Newton-Raphson method to find the solution. Solution of (3.3) is not as straightforward in general when $\mathbf{Q}(t)$ is not a polynomial spiral segment; solution of (3.3) for some non-polynomial spiral segments are considered in the next section.

For a polynomial spiral segment of degree n, Eqn. (3.3) is equivalent to

$$\mu g_i(t) = 0, \quad i = 0, 1,$$

where μ is a constant,

$$g_i(t) = \sum_{j=0}^{m} \alpha_{i,j} t^j, \quad min(t_i, \eta) \leq t \leq max(t_i, \eta), \tag{3.6}$$

$m = 2n - 1$, and $\alpha_{i,j}, j = 0, \cdots, m$ depend on $\mathbf{Q}(t)$. Expressions for the $\alpha_{i,j}$'s are derived in Chapter 4 for some polynomial spiral segments. Since (3.5) is satisfied for $t = t_i, g_i(t)$ it follows that

$$0 = \sum_{j=0}^{m} \alpha_{i,j} t_i^j. \tag{3.7}$$

Subtraction of (3.6) from (3.5) yields

$$g_i(t) = \alpha_{i,1}(t - t_i) + \alpha_{i,2}(t^2 - t_i^2) + \cdots + \alpha_{i,m-1}(t^{m-1} - t_i^{m-1}) + \alpha_{i,m}(t^m - t_i^m)$$

or, factoring differences of powers of t,

$$\begin{aligned} g_i(t) &= (t - t_i)\alpha_{i,1} + (t - t_i)\alpha_{i,2}(t + t_i) + (t - t_i)\alpha_{i,3}(t^2 + tt_i + t_i^2) + \cdots \\ &\quad + (t - t_i)\alpha_{i,m}(t^{m-1} + t^{m-2}t_i + \cdots + t_i^{m-1}). \end{aligned}$$

hence,

$$g_i(t) = (t - t_i)q_i(t),$$

where

$$\begin{aligned} q_i(t) &= \alpha_{i,1} + \alpha_{i,2}(t + t_i) + \alpha_{i,3}(t^2 + tt_i + t_i^2) + \cdots \\ &\quad + \alpha_{i,m-1}(t^{m-2} + t^{m-3}t_i + \cdots + t_i^{m-2}) + \alpha_{i,m}(t^{m-1} + t^{m-2}t_i + \cdots + t_i^{m-1}). \end{aligned}$$

which is the same as,

$$q_i(t) = \sum_{j=1}^{m}\sum_{k=0}^{j-1} \alpha_{i,j} t_i^{j-k-1} t^k$$

Regrouping the terms according to the nominal of t and rewriting them by increasing order of t,

$$\begin{aligned} q_i(t) &= \alpha_{i,1} + \alpha_{i,2}t_i + \alpha_{i,3}t_i^2 + \cdots + \alpha_{i,m}t_i^{m-1} \\ &\quad + t(\alpha_{i,2} + \alpha_{i,3}t_i + \cdots + +\alpha_{i,m}t_i^{m-2}) + \cdots \\ &\quad + t^{m-2}(\alpha_{i,m-1} + \alpha_{i,m}t_i) + t^{m-1}\alpha_{i,m} \end{aligned}$$

which can be written as,

$$q_i(t) = \sum_{k=0}^{m-1}\sum_{j=k+1}^{m} \alpha_{i,j} t_i^{j-k-1} t^k. \tag{3.8}$$

Eqn. (3.3) can be solved by applying numerical techniques to $q_i(t) = 0$ where $q_i(t)$ is given in Eqn.(3.7). Note that it does not contain $\alpha_{i,0}$.

3.2.2 Other Spiral Segments

The problem here is how to factor t_i out because it is a solution but not the one which is sought. Since the clothoid, logarithmic and Archimedean spirals are not polynomial, it is difficult to factor t_i out.

Considering that $g_i(t) = \mu\{\mathbf{Q}(t) - \mathbf{C}_i\} \cdot \mathbf{Q}'(t)$ has at least one solution but no more than two solutions in $[t_0, \eta]$ or $[\eta, t_1]$, there is at most one solution in (t_0, η) or (η, t_1) since t_i $(i = 0, 1)$ satisfies $g_i(t) = 0$. Fig. (3.3) and Fig. (3.4) show the only two possible ways of the solution: it appears in the interval or not. Observe that t_0 is the beginning point of one interval containing a possible solution and t_1 is the ending point of another interval containing a possible solution; $\mathbf{Q}(\eta)$ is the point on the spiral where the normal vector of the biarc at its joint intersects the spiral. Since the sign of $g_i(t)$ depends on whether the counter-clockwise angle from vector $\mathbf{Q}(t) - \mathbf{C}_i$ to vector $\mathbf{Q}'(t)$ is bigger than $\pi/2$ or not, there are two curves in each diagram to represent these two different cases. Fig.(3.3) shows the case when $t = t_0$ or t_1 is the only value that satisfies that $g_i(t) = 0$ when $t \in [t_0, \eta)$ or $t \in (\eta, t_1]$. Fig.(3.4) shows the case when another solution is included in that range.

In order to check if the solution is in the interval (t_0, η) or (η, t_1), test the sign of $g_i'(t_0)g_i(\eta)$ or $g_i'(t_1)g_i(\eta)$.

- In the interval $t \in (t_0, \eta)$:

  Suppose $g_i(s) = 0$, as in Fig. (3.3) (a) or Fig. (3.4) (a). If s is not in (t_0, η) then $g_i'(t_0)g(\eta) > 0$ and if $s \in (t_0, \eta)$ then $g_i'(t_0)g(\eta) < 0$.

- In the interval $t \in (\eta, t_i)$:

  Suppose $g_i(s) = 0$, as in Fig. (3.3) (b) or Fig. (3.4) (b). If s is not in (η, t_1)

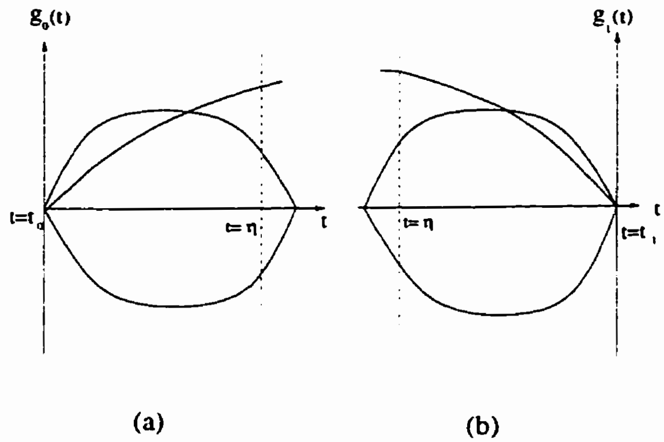

Figure 3.3: Plot of $g_i(t)$

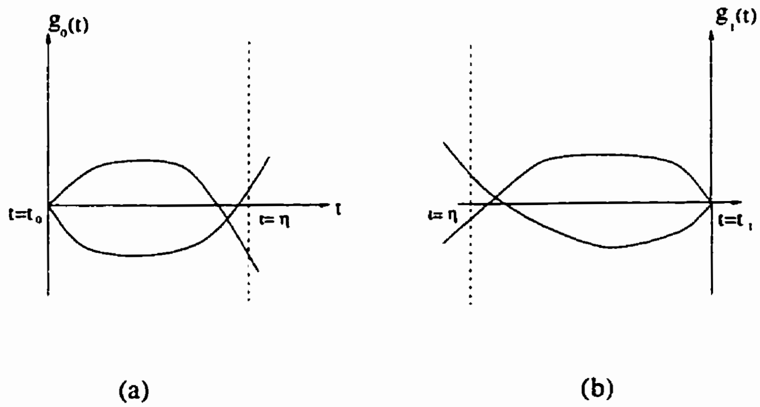

Figure 3.4: Plot of $g_i(t)$

then $g_i'(t_1)g(\eta) < 0$ and if $s \in (\eta, t_1)$ then $g_i'(t_1)g(\eta) > 0$.

In case $g_i'(t_0)$ or $g_i'(t_1)$ is zero, the second derivative can be used to judge the tendency of $g_i(t_i)$. If a solution is known to be between η and t_i ($i = 0, 1$), the bisection method can be used to locate the solution. If there is no solution between η and t_i, then the maximum deviation occurs at $t = \eta$. Notice that even if $g_i(t)$ is bumpy as in Fig. (3.5), the check is still applicable, since there is at most one solution.

Theoretically, one may omit t_i easily, but when using a numerical method, it is not easy to decide on which range bisection should be applied. It is known that η is one of the end points, but how close to t_i should the other end point be? If it is known that there is a solution other than $t = t_i$ $(i = 0, 1)$ in $[t_0, \eta]$ or $[\eta, t_1]$, then recursive subdivision can be used to find an interval in which it is certain that the solution is contained. In practice, subdividing only once usually works.

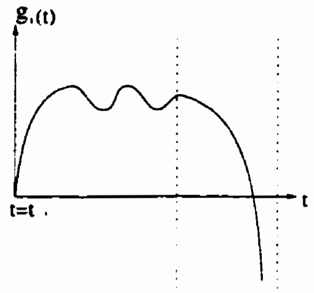

Figure 3.5: Bumps Appear.

Chapter 4

Spirals

In Chapter 3, a spiral segment that is expressed by a mathematical formula is approximated by a biarc. A general idea was presented to approximate a spiral segment given by a mathematical expression. Since the approximating biarc is determined only by the given beginning point, the ending point and tangential direction at these points, the formula for maximum deviation between a spiral and the corresponding biarc varies from spiral to spiral and one free parameter. It does not seem possible to find a general mathematical expression for the deviation that can be evaluated economically in practice. In this chapter, the deviation will be examined for individual spirals such as PH cubic, PH quintic, clothoidal, Archimedean and logarithmic. The deviation results of quadratic and cubic Bézier are available in the literature, but will be restated for comparison. A practical method will be developed to solve the equations. Numerical methods are used to solve polynomial and other non-linear equations.

4.1 Quadratic Bézier Spiral

In Walton and Meek's paper [WM94], three theorems are stated. The first one proves that a unique biarc can be constructed given the control vertices by choosing the joint at the incentre of the control triangle according to the method suggested by Sabin. The other two theorems are presented to determine the maximum deviation from the spiral to the corresponding biarc. In the second theorem, the coordinate system is adjusted by setting the origin at $\mathbf{G}$, the joint of two arcs. The y-axis is along the normal direction at $\mathbf{G}$. Under the new coordination system, the curve has expression $(x(t), y(t))$, The deviation at the joint is equal to $y(t)$ when $x(t) = 0$. The other theorem is applied to determine the local extreme deviation for a specific arc of the two circular arcs. The maximum deviation is determined by comparing these extrema.

Actually, the method mentioned in chapter 3 can be applied in this case and it will lead to the result in [WM94] with a more generalized form. Notice that the interval of t in all Bézier curves analyzed here is from 0 to 1 due to its definition. From Eqn. (2.14) and (2.15), the quadratic Bézier spiral segment and its first derivative can be written as

$$\mathbf{Q}(t) = \mathbf{P}_0 + 2a\mathbf{T}_0 t + (b\mathbf{T}_1 - a\mathbf{T}_0)t^2 \tag{4.1}$$

and

$$\mathbf{Q}'(t) = 2\{a\mathbf{T}_0 + (b\mathbf{T}_1 - a\mathbf{T}_0)t\} \tag{4.2}$$

respectively.

Substitution of Eqn. (4.1) and (4.2) into Eqn. (3.3) gives

$$\left\{\mathbf{P}_0 - \mathbf{C}_i + 2a\mathbf{T}_0 t + (b\mathbf{T}_1 - a\mathbf{T}_0)t^2\right\} \bullet \left\{a\mathbf{T}_0 + (b\mathbf{T}_1 - a\mathbf{T}_0)t\right\} = 0$$

The above equation can be put in the form of Eqn. (3.7) where,

$$\begin{aligned}
m &= 3, \\
\alpha_{i,0} &= a(\mathbf{P}_0 - \mathbf{C}_i) \cdot \mathbf{T}_0, \\
\alpha_{i,1} &= 2a^2 + (\mathbf{P}_0 - \mathbf{C}_i) \cdot (b\mathbf{T}_1 - a\mathbf{T}_0), \qquad (4.3) \\
\alpha_{i,2} &= 3a(b\mathbf{T}_0 \cdot \mathbf{T}_1 - a) \\
\alpha_{i,3} &= (a^2 - 2ab\mathbf{T}_0 \cdot \mathbf{T}_1 + b^2).
\end{aligned}$$

4.2 Cubic Bézier Spiral

Results for the cubic spiral segment are available in Walton and Meek's paper [WM96c]. The results are summarized below.

$$\mathbf{Q}(t) = \mathbf{P}_0 + 3a\mathbf{T}_0 t + (b\mathbf{T}_1 - a\mathbf{T}_0)t^3 \qquad (4.4)$$

and

$$\mathbf{Q}'(t) = 3a\mathbf{T}_0 + 3(b\mathbf{T}_1 - a\mathbf{T}_0)t^2, \quad 0 \leq t \leq 1, \qquad (4.5)$$

where a and b are defined in Eqn.(2.12). After applying Eqn.(4.4) and (4.5), (3.3) can be put in the form of Eqn.(3.7) where,

$$\begin{aligned}
m &= 5, \\
\alpha_{i,0} &= 3a\mathbf{T}_0 \cdot (\mathbf{P}_0 - \mathbf{C}_i), \\
\alpha_{i,1} &= 3a^2, \\
\alpha_{i,2} &= (\mathbf{P}_0 - \mathbf{C}_i) \cdot (b\mathbf{T}_1 - a\mathbf{T}_0), \qquad (4.6) \\
\alpha_{i,3} &= 4a(b\mathbf{T}_0 \cdot \mathbf{T}_1 - a)
\end{aligned}$$

$$
\begin{aligned}
\alpha_{i,4} &= 0 \\
\alpha_{i,5} &= a^2 - 2ab\mathbf{T}_0 \cdot \mathbf{T}_1 + b^2.
\end{aligned}
$$

4.3 PH Cubic Spiral

Expanding Eqn. (2.23) in power form gives

$$
\begin{aligned}
\mathbf{Q}(t) &= \mathbf{P}_0 + (\mathbf{P}_1 - 3\mathbf{P}_0)t + (\mathbf{P}_2 - 2\mathbf{P}_1 + 3\mathbf{P}_0)t^2 \\
&\quad + (\mathbf{P}_3 - \mathbf{P}_2 + \mathbf{P}_1 - \mathbf{P}_0)t^3.
\end{aligned}
$$

Since $\mathbf{P}_1, \mathbf{P}_2, \mathbf{P}_3$ can be expressed in terms of $\mathbf{P}_0, u_0, u_1, v_0, v_1$ from Eqn.(2.27), the above can also be written as

$$
\begin{aligned}
\mathbf{Q}(t) &= \mathbf{P}_0 + u_0^2\mathbf{T}_0 t + [u_0(u_1 - u_0)\mathbf{T}_0 + u_0 v_1 \mathbf{N}_0]t^2 \\
&\quad + \frac{1}{3}\{[(u_1 - u_0)^2 - v_1^2]\mathbf{T}_0 + 2v_1(u_1 - u_0)\mathbf{N}_0\}t^3 \qquad (4.7)
\end{aligned}
$$

$$
\begin{aligned}
\mathbf{Q}'(t) &= u_0^2\mathbf{T}_0 + 2u_0[(u_1 - u_0)\mathbf{T}_0 + v_1\mathbf{N}_0]t \\
&\quad + \{[(u_1 - u_0)^2 - v_1^2]\mathbf{T}_0 + 2v_1(u_1 - u_0)\mathbf{N}_0\}t^2 \qquad (4.8)
\end{aligned}
$$

Substitutions of Eqns. (4.7) and (4.8) into function $g_i(t)$(Eqn.(3.3)) gives

$$
\begin{aligned}
g_i(t) &= \Big\{\mathbf{P}_0 - \mathbf{C}_i + u_0^2\mathbf{T}_0 t + [u_0(u_1 - u_0)\mathbf{T}_0 + u_0 v_1 \mathbf{N}_0]t^2 \\
&\quad + \frac{1}{3}\{[(u_1 - u_0)^2 - v_1^2]\mathbf{T}_0 + 2v_1(u_1 - u_0)\mathbf{N}_0\}t^3\Big\} \bullet \\
&\quad \Big\{u_0^2\mathbf{T}_0 + 2u_0[(u_1 - u_0)\mathbf{T}_0 + v_1\mathbf{N}_0]t \\
&\quad + \{[(u_1 - u_0)^2 - v_1^2]\mathbf{T}_0 + 2v_1(u_1 - u_0)\mathbf{N}_0\}t^2\Big\}
\end{aligned}
$$

or after expansion and re-arrangement, it can be adjusted to the form of Eqn. (3.7), with

$$m = 5$$

$$\begin{aligned}
\alpha_{i,0} &= u_0^2(\mathbf{P}_0 - \mathbf{C}_i) \cdot \mathbf{T}_0 \\
\alpha_{i,1} &= u_0^4 + 2u_0(\mathbf{P}_0 - \mathbf{C}_i) \cdot [(u_1 - u_0)\mathbf{T}_0 + v_1\mathbf{N}_0] \\
\alpha_{i,2} &= (\mathbf{P}_0 - \mathbf{C}_i) \cdot \{[(u_1 - u_0)^2 - v_1^2]\mathbf{T}_0 + 2v_1(u_1 - u_0)\mathbf{N}_0\} + 3u_0^3(u_1 - u_0) \\
\alpha_{i,3} &= \frac{2}{3}u_0^2[5(u_1 - u_0)^2 + v_1^2] \qquad (4.9) \\
\alpha_{i,4} &= \frac{5}{3}u_0(u_1 - u_0)[(u_1 - u_0)^2 + v_1^2] \\
\alpha_{i,5} &= \frac{1}{3}[(u_1 - u_0)^2 + v_1^2]^2
\end{aligned}$$

4.4 PH Quintic Spiral

Expanding Eqn.(1.2) with $n = 5$ in power form gives

$$\begin{aligned}
\mathbf{Q}(t) &= \mathbf{P}_0 + (4\mathbf{P}_1 - 5\mathbf{P}_0)t + (6\mathbf{P}_2 - 16\mathbf{P}_1 + 10\mathbf{P}_0)t^2 \\
&\quad +(\mathbf{P}_3 - 18\mathbf{P}_2 + 24\mathbf{P}_1 - 10\mathbf{P}_0)t^3 \\
&\quad +(\mathbf{P}_4 - 2\mathbf{P}_3 + 18\mathbf{P}_2 - 16\mathbf{P}_1 + 5\mathbf{P}_0)t^4 \\
&\quad +(\mathbf{P}_5 - \mathbf{P}_4 + \mathbf{P}_3 - 6\mathbf{P}_2 + 4\mathbf{P}_1 - \mathbf{P}_0)t^5
\end{aligned}$$

Since $\mathbf{P}_1, \mathbf{P}_2, \mathbf{P}_3, \mathbf{P}_4, \mathbf{P}_5$ can be expressed in terms of $\mathbf{P}_0, u_0, u_1, v_0, v_1$ from Eqn.(2.35), the above can also be written as

$$\begin{aligned}
\mathbf{Q}(t) &= \mathbf{P}_0 + u_0^2\mathbf{T}_0 t + \frac{2}{3}u_0[(u_2 - u_0)\mathbf{T}_0 + v_2\mathbf{N}_0]t^3 \\
&\quad +\frac{1}{5}\{[(u_2 - u_0)^2 - v_2^2]\mathbf{T}_0 + 2v_2(u_2 - u_0)\mathbf{N}_0\}t^5 \qquad (4.10)
\end{aligned}$$

$$\begin{aligned} \mathbf{Q}'(t) &= u_0^2\mathbf{T}_0 + 2u_0[(u_2-u_0)\mathbf{T}_0 + v_2\mathbf{N}_0]t^2 \\ &\quad +\{[(u_2-u_0)^2 - v_2^2]\mathbf{T}_0 + 2v_2(u_2-u_0)\mathbf{N}_0\}t^4 \end{aligned} \tag{4.11}$$

From (2.2) and (2.3) the function $g_i(t)$may be written as

$$\begin{aligned} g_i(t) &= \Big\{\mathbf{P}_0 - \mathbf{C}_i + u_0^2\mathbf{T}_0 t + \frac{2}{3}u_0[(u_2-u_0)\mathbf{T}_0 + v_2\mathbf{N}_0]t^3 \\ &\quad +\frac{1}{5}\{[(u_2-u_0)^2 - v_2^2]\mathbf{T}_0 + 2v_2(u_2-u_0)\mathbf{N}_0\}t^5\Big\} \bullet \\ &\quad \Big\{u_0^2\mathbf{T}_0 + 2u_0[(u_2-u_0)\mathbf{T}_0 + v_2\mathbf{N}_0]t^2 \\ &\quad +\{[(u_2-u_0)^2 - v_2^2]\mathbf{T}_0 + 2v_2(u_2-u_0)\mathbf{N}_0\}t^4\Big\} \end{aligned}$$

or after expansion and re-arrangement, it can be regrouped into the form of Eqn. (3.7), with

$$m = 9$$

$$\begin{aligned} \alpha_{i,0} &= u_0^2(\mathbf{P}_0 - \mathbf{C}_i)\cdot\mathbf{T}_0 \\ \alpha_{i,1} &= u_0^4 \\ \alpha_{i,2} &= 2u_0(\mathbf{P}_0 - \mathbf{C}_i)\cdot[(u_2-u_0)\mathbf{T}_0 + v_2\mathbf{N}_0] \\ \alpha_{i,3} &= \frac{8}{3}u_0^3(u_2-u_0) \\ \alpha_{i,4} &= (\mathbf{P}_0 - \mathbf{C}_i)\cdot\{[(u_2-u_0)^2 - v_2^2]\mathbf{T}_0 + 2v_2(u_2-u_0)\mathbf{N}_0\} \\ \alpha_{i,5} &= \frac{2}{15}u_0^2[19(u_2-u_0)^2 + v_2^2] \\ \alpha_{i,6} &= 0 \\ \alpha_{i,7} &= \frac{16}{15}u_0(u_2-u_0)[(u_2-u_0)^2 + v_2^2] \\ \alpha_{i,8} &= 0 \\ \alpha_{i,9} &= \frac{1}{5}[(u_2-u_0)^2 + v_2^2]^2. \end{aligned} \tag{4.12}$$

4.5 Clothoid

The clothoidal spiral (or Cornu Spiral) can be expressed as

$$\mathbf{Q}(t) = \mathbf{P}_0 + aC(t)\mathbf{T}_0 + aS(t)\mathbf{N}_0 \tag{4.13}$$

where a is a constant. The first derivative of this function is:

$$\mathbf{Q}'(t) = a\cos\frac{\pi t^2}{2}\mathbf{T}_0 + a\sin\frac{\pi t^2}{2}\mathbf{N}_0 \tag{4.14}$$

To approximate a piece of the clothoidal spiral segment with $t \in [t_0, t_1]$, a triangle can be built by $\mathbf{Q}(t_0)$, $\mathbf{Q}(t_1)$, $\mathbf{Q}'(t_0)$ and $\mathbf{Q}'(t_1)$. Suppose the incentre of the triangle is $\mathbf{G}$ where the two arcs join and the centre of the two arcs are $\mathbf{C}_i$ $(i = 0, 1)$. Replacing $\mathbf{Q}(t)$ and $\mathbf{Q}'(t)$ in Eqn. (3.3), the function $g_i(t)$ may be written as

$$g_i(t) = \left(\mathbf{P}_0 - \mathbf{C}_i + aC(t)\mathbf{T}_0 + aS(t)\mathbf{N}_0\right) \bullet \left(a\cos\frac{\pi t^2}{2}\mathbf{T}_0 + a\sin\frac{\pi t^2}{2}\mathbf{N}_0\right). \tag{4.15}$$

Simplification of Eqn.(4.15) using $\mathbf{T}_0 \cdot \mathbf{N}_0 = 0$ gives

$$g_i(t) = [(\mathbf{P}_0 - \mathbf{C}_i)\cdot\mathbf{T}_0 + aC(t)]a\cos\frac{\pi}{2}t^2 + [(\mathbf{P}_0 - \mathbf{C}_i)\cdot\mathbf{N}_0 + aS(t)]a\sin\frac{\pi}{2}t^2 \tag{4.16}$$

The solution to equation $g_i(t) = 0$ is the local maxima of the deviation.

For the clothoid spiral, the first derivative of $g_i(t)$ can be obtained from Eqn.(4.16) as

$$\begin{aligned} g_i'(t) \quad = \quad & a\{aC'(t)\cos\frac{\pi}{2}t^2 - [(\mathbf{P}_0 - \mathbf{C}_i)\cdot\mathbf{T}_0 + aC(t)]\pi t\sin\frac{\pi t^2}{2} + \\ & aS'(t)\sin\frac{\pi}{2}t^2 + [(\mathbf{P}_0 - \mathbf{C}_i)\cdot\mathbf{N}_0 + aS(t)]\pi t\cos\frac{\pi t^2}{2}\} \end{aligned}$$

Note that $C'(t)\cos\frac{\pi}{2}t^2 + S'(t)\sin\frac{\pi}{2}t^2 = 1$. So,

$$\begin{aligned} g_i'(t) \quad = \quad & -\pi at\{[(\mathbf{P}_0 - \mathbf{C}_i)\cdot\mathbf{T}_0 + aC(t)]\sin\frac{\pi t^2}{2} - \\ & [(\mathbf{P}_0 - \mathbf{C}_i)\cdot\mathbf{N}_0 + aS(t)]\cos\frac{\pi t^2}{2}\} + a^2 \end{aligned} \tag{4.17}$$

4.6 Archimedean Spiral

Referring to Eqn. (2.54), the Archimedean spiral can be expressed as

$$\mathbf{Q}(t) = \mathbf{P}_0 + at^{\frac{1}{m}} \cos t\mathbf{T}_0 + at^{\frac{1}{m}} \sin t\mathbf{N}_0 \tag{4.18}$$

where a and m are constants. The first derivative of the Archimedean spiral function is

$$\mathbf{Q}'(t) = (\frac{a}{m}t^{\frac{1}{m}-1} \cos t - at^{\frac{1}{m}} \sin t)\mathbf{T}_0 + (\frac{a}{m}t^{\frac{1}{m}-1} \sin t + at^{\frac{1}{m}} \cos t)\mathbf{N}_0 \tag{4.19}$$

To approximate Archimedean spiral segment with $t \in [t_0, t_1]$, a triangle can be built by $\mathbf{Q}(t_0)$, $\mathbf{Q}(t_1)$, $\mathbf{Q}'(t_0)$ and $\mathbf{Q}'(t_1)$. Suppose the incentre of the triangle is $\mathbf{G}$ where the two arcs join and the centre of the two arcs are $\mathbf{C}_i$ $(i = 0, 1)$. Replacing $\mathbf{Q}(t)$ and $\mathbf{Q}'(t)$ in Eqn. (3.3), the function $g_i(t)$ may be written as

$$\begin{aligned} g_i(t) &= \left[\mathbf{P}_0 - \mathbf{C}_i + at^{\frac{1}{m}} \cos t\mathbf{T}_0 + at^{\frac{1}{m}} \sin t\mathbf{N}_0\right] \bullet \\ &\quad \left[(\frac{a}{m}t^{\frac{1}{m}-1} \cos t - at^{\frac{1}{m}} \sin t)\mathbf{T}_0 + (\frac{a}{m}t^{\frac{1}{m}-1} \sin t + at^{\frac{1}{m}} \cos t)\mathbf{N}_0\right] \end{aligned} \tag{4.20}$$

Simplification of Eqn. (4.20) using $\mathbf{T}_0 \cdot \mathbf{N}_0 = 0$ gives

$$\begin{aligned} g_i(t) &= \frac{a^2}{m}t^{\frac{2}{m}-1} + (\mathbf{P}_0 - \mathbf{C}_i) \cdot \mathbf{T}_0(\frac{a}{m}t^{\frac{1}{m}-1} \cos t - at^{\frac{1}{m}} \sin t) \\ &+ (\mathbf{P}_0 - \mathbf{C}_i) \cdot \mathbf{N}_0(\frac{a}{m}t^{\frac{1}{m}-1} \sin t + at^{\frac{1}{m}} \cos t) \end{aligned} \tag{4.21}$$

The local maxima of the deviation are given by the solution to $g_i(t) = 0$. The method for solving non-polynomial equations introduced in section (3.2.2) can be applied here. The derivative of $g_i(t)$ is useful in solving the equation,

$$\begin{aligned} g_i'(t) &= \frac{a^2}{m^2}(2 - m)t^{\frac{2}{m}-2} + (\mathbf{P}_0 - \mathbf{C}_i) \cdot \mathbf{T}_0 at^{\frac{1}{m}}(\frac{1 - m}{m^2t^2} \cos t - \frac{2}{mt} \sin t - \cos t) \\ &+ (\mathbf{P}_0 - \mathbf{C}_i) \cdot \mathbf{N}_0 at^{\frac{1}{m}}(\frac{1 - m}{m^2t^2} \sin t + \frac{2}{mt} \cos t - \sin t) \end{aligned} \tag{4.22}$$

4.7 Logarithmic Spiral

As shown in Eqn. (2.59), the logarithmic spiral can be expressed as

$$\begin{aligned}\mathbf{Q}(t) &= \mathbf{P}_0 + \frac{1}{c_0(k^2+1)}\{[e^{kt}(k\cos t + \sin t) - k]\mathbf{T}_0 \\ &\quad + [e^{kt}(k\sin t - \cos t) + 1]\mathbf{N}_0\}, \quad 0 \le t \le \theta. \qquad (4.23)\end{aligned}$$

where c_0 is the curvature of the starting point and $k = \frac{ln\frac{c_0}{c}}{\theta}$. The first derivative of $\mathbf{Q}(t)$ is:

$$\mathbf{Q}'(t) = \frac{e^{kt}}{c_0}(\cos t\mathbf{T}_0 + \sin t\mathbf{N}_0), \quad 0 \le t \le \theta. \qquad (4.24)$$

To approximate logarithmic spiral segment with $t \in [t_0, t_1]$, a triangle can be built by $\mathbf{Q}(t_0)$, $\mathbf{Q}(t_1)$, $\mathbf{Q}'(t_0)$ and $\mathbf{Q}'(t_1)$. Suppose the incentre of the triangle is $\mathbf{G}$ where the two arcs join and the centre of the two arcs are $\mathbf{C}_i$ $(i = 0, 1)$. Replacing $\mathbf{Q}(t)$ and $\mathbf{Q}'(t)$ into Eqn. (3.3), the function $g_i(t)$ may be written as

$$\begin{aligned}g_i(t) &= \Big\{\mathbf{P}_0 - \mathbf{C}_i + \frac{1}{c_0(k^2+1)}\{[e^{kt}(k\cos t + \sin t) - k]\mathbf{T}_0 \\ &\quad + [e^{kt}(k\sin t - \cos t) + 1]\mathbf{N}_0\}\Big\} \bullet \Big\{\frac{e^{kt}}{c_0}[(\cos t)\mathbf{T}_0 + (\sin t)\mathbf{N}_0]\Big\} \qquad (4.25)\end{aligned}$$

Simplification of Eqn. (4.25) using $\mathbf{T}_0 \cdot \mathbf{N}_0 = 0$ yields

$$g_i(t) = \frac{e^{kt}}{c_0}(\mathbf{P}_0 - \mathbf{C}_i) \cdot [(\cos t)\mathbf{T}_0 + (\sin t)\mathbf{N}_0] + \frac{e^{kt}}{c_0^2(k^2+1)}(ke^{kt} - k\cos t + \sin t) \qquad (4.26)$$

The solutions to $g_i(t) = 0$ give the local maxima of the deviation. The method mentioned in section (3.2.2) can be applied to solve the equation. The derivative of $g_i(t)$ is useful in solving the equation,

$$\begin{aligned}g_i'(t) &= \frac{e^{kt}}{c_0}(\mathbf{P}_0 - \mathbf{C}_i) \cdot (-\sin t\mathbf{T}_0 + \cos t\mathbf{N}_0) + \frac{ke^{kt}}{c_0}(\mathbf{P}_0 - \mathbf{C}_i) \cdot (\cos t\mathbf{T}_0 + \sin t\mathbf{N}_0) \\ &\quad + \frac{ke^{kt}}{c_0^2(k^2+1)}(ke^{kt} - k\cos t + \sin t) + \frac{e^{kt}}{c_0^2(k^2+1)}(k^2e^{kt} + k\sin t + \cos t)\end{aligned}$$

$$
\begin{aligned}
&= \frac{e^{kt}}{c_0}(\mathbf{P}_0 - \mathbf{C}_i) \cdot \Big[(k\cos t - \sin t)\mathbf{T}_0 + (k\sin t - \cos t)\mathbf{N}_0\Big] \\
&\quad + \frac{e^{kt}}{c_0^2(k^2+1)}\Big[2k^2 e^{kt} + (1-k^2)\cos t + 2k\sin t\Big] \qquad (4.27)
\end{aligned}
$$

Chapter 5

Algorithms

In this chapter, some geometry formulae are introduced for the convenience of generating algorithms. Pseudo-code of the algorithms which are based on the theorems illustrated in Chapter 3 and Chapter 4 is presented.

It uses the well-known geometric facts that:

Given three points $\mathbf{A}$, $\mathbf{B}$ and $\mathbf{C}$, $\| \mathbf{AB} \| = \| \mathbf{BC} \| = b$, $\| \mathbf{AC} \| = c$, as shown in Fig. (5.1),

Fact5.1 A unique circle can be found, so that it goes through $\mathbf{A}$, $\mathbf{C}$ and is tangent at these two points to $\mathbf{AB}$ and $\mathbf{BC}$, respectively.

Fact5.2 The radius of the circle is $r = \frac{bc}{\sqrt{4b^2 - c^2}}$.

To facilitate the computation of the incentre of a triangle by vectors, *Lemma* 5.1 gives the ratio of $\| \mathbf{A}_0\mathbf{W}_0 \|$ and $\| \mathbf{A}_0\mathbf{A}_1 \|$ in terms of cosines of the angles of the triangle as shown in Fig.(5.2). The result can thus be expressed using inner products.

Lemma 5.1 Given a $\triangle \mathbf{A}_0\mathbf{A}_1\mathbf{A}_2$ as shown in Fig.(5.2), where $\mathbf{G}$ is the incentre of the triangle. Suppose $\angle \mathbf{A}_1\mathbf{A}_0\mathbf{A}_2 = \alpha$ and $\angle \mathbf{A}_0\mathbf{A}_1\mathbf{A}_2 = \beta$ Through $\mathbf{G}$ draw a line

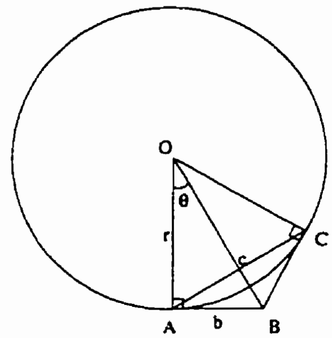

Figure 5.1: Circle Determined by an Isosceles Triangle

$\mathbf{W_0W_1}$ which is parallel to $\mathbf{A_0A_1}$, then

(a) $\| \mathbf{A_0W_0} \| = \| \mathbf{GW_0} \|$, $\| \mathbf{GW_1} \| = \| \mathbf{A_1W_1} \|$.

(b) $\frac{\|\mathbf{A_0W_0}\|}{\|\mathbf{A_0A_1}\|} = \frac{\cos(\frac{\pi}{2}-\beta)}{\cos(\frac{\pi}{2}-\alpha-\beta)+\cos(\frac{\pi}{2}-\beta)+\cos(\frac{\pi}{2}-\alpha)}$

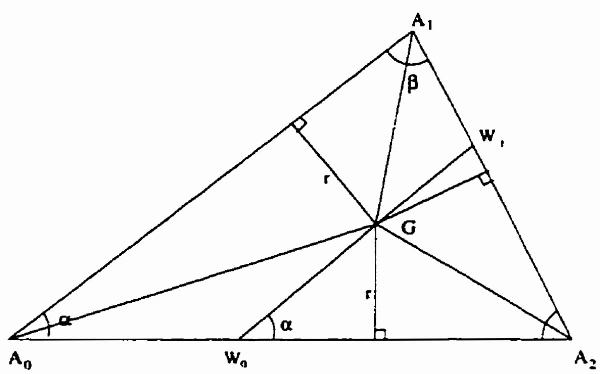

Figure 5.2: Incentre of Triangle

Proof:

Equations (a) are obvious since $\mathbf{GA_0}$ bisects α and $\mathbf{W_0W_1} \parallel \mathbf{A_0A_1}$; these conditions lead to $\angle\mathbf{GA_0W_0} = \angle\mathbf{A_0GW_0}$; so $\triangle\mathbf{A_0GW_0}$ is an isosceles triangle with $\| \mathbf{A_0W_0} \| = \| \mathbf{GW_0} \|$. Similarly $\| \mathbf{GW_1} \| = \| \mathbf{A_1W_1} \|$.

Suppose the radius of the inscribed circle is r. From Fig. (5.2),

$$\| \mathbf{A}_0\mathbf{A}_1 \| = \frac{r}{\tan\frac{\alpha}{2}} + \frac{r}{\tan\frac{\beta}{2}},$$

and

$$\| \mathbf{A}_0\mathbf{W}_0 \| = \frac{r}{\tan\frac{\alpha}{2}} - \frac{r}{\tan\alpha}.$$

So,

$$\frac{\| \mathbf{A}_0\mathbf{W}_0 \|}{\| \mathbf{A}_0\mathbf{A}_1 \|} = \frac{\frac{1}{\tan\frac{\alpha}{2}} - \frac{1}{\tan\alpha}}{\frac{1}{\tan\frac{\alpha}{2}} + \frac{1}{\tan\frac{\beta}{2}}}$$

It is known that $\tan\frac{\alpha}{2} = \frac{\sin\alpha}{1+\cos\alpha}$, hence

$$\frac{\| \mathbf{A}_0\mathbf{W}_0 \|}{\| \mathbf{A}_0\mathbf{A}_1 \|} = \frac{\frac{1}{\tan\frac{\alpha}{2}} - \frac{1}{\tan\alpha}}{\frac{1}{\tan\frac{\alpha}{2}} + \frac{1}{\tan\frac{\beta}{2}}} = \frac{1 - \frac{\tan\frac{\alpha}{2}}{\tan\alpha}}{1 + \frac{\tan\frac{\alpha}{2}}{\tan\frac{\beta}{2}}}$$

$$\begin{aligned}
&= \frac{1 - \frac{\sin\alpha}{1+\cos\alpha}\frac{\cos\alpha}{\sin\alpha}}{1 + \frac{\sin\alpha}{1+\cos\alpha}\frac{1+\cos\beta}{\sin\beta}} \\
&= \frac{(1+\cos\alpha-\cos\alpha)\sin\beta}{(1+\cos\alpha)\sin\beta + \sin\alpha(1+\cos\beta)} \\
&= \frac{\sin\beta}{\sin(\alpha+\beta)+\sin\beta+\sin\alpha} \square
\end{aligned}$$

5.1 Algorithm

The algorithm is based on recursive subdivision of a spiral segment until each subpart of the segment may be approximated by a biarc within a given tolerance τ. Subdivision occurs at the point of maximum deviation of the spiral from the approximating biarc. The deviation is measured along a radial direction of the biarc. The algorithm is presented in pseudocode.

The parameter $\mathbf{P}_0$ is the beginning point of a given spiral segment and $\mathbf{T}_0$ is the unit tangent of the spiral at this point. Parameter c is the ending curvature.

The quantity θ is the angle between $\mathbf{T}_0$ and the unit tangent of the ending point of the spiral segment. For polynomial and clothoidal spiral segments, a unique spiral segment can be determined given $\mathbf{P}_0$, $\mathbf{T}_0$, θ and c. For Archimedean spiral segment parameter $\mathbf{P}_0$, $\mathbf{T}_0$, t_0 and t_1 are to be specified. For logarithmic spiral segment $\mathbf{P}_0$, $\mathbf{T}_0$, θ , c and the initial curvature c_0 should be given. The algorithm is described in terms of ten modules called procedures.

Procedure InitParameter initializes the parameter for each spiral segment by generating *spiral_data*. Procedures EvalQ and EvalDQ are used to evaluate the spiral and its first derivative respectively at a point. Function FindBiArcTri is used to construct a triangle defined by two points, $\mathbf{A}_0$, $\mathbf{A}_1$ on the spiral and its corresponding unit tangent vectors $\mathbf{H}_0$, $\mathbf{H}_1$ at those points, as shown in Fig. (5.3). FitBiArc is called to find the location of $\mathbf{W}_0$, $\mathbf{G}$ and $\mathbf{W}_1$ (Fig 5.3) using *Lemma* 5.1. FindArc is called to determine two arcs given $\mathbf{A}_0$, $\mathbf{W}_0$, $\mathbf{G}$ and $\mathbf{G}$, $\mathbf{W}_1$, $\mathbf{A}_1$ by using Fact 5.1 and 5.2. DevAtJoint is called to compute the radial deviation at the joint. MaxDevP and MaxDevNP are called for polynomial equations and non polynomial equations respectively to compute the possible local maxima on either one of the arcs. The bisection method is used to find the solution if the local maxima appear. In these two procedures t_i $(i = 0, 1)$ is the parameter at the beginning or ending point of the current spiral segment and η is the parameter where the radial direction at the joint of the biarc intersects with the spiral segment. Procedure ApproxSpiral is used to approximate a single segment.

Procedure InitParameter($\mathbf{P}_0$, $\mathbf{T}_0$, c, c_0, θ, t_0, t_1)

Switch (spiral) {

case quadratic:

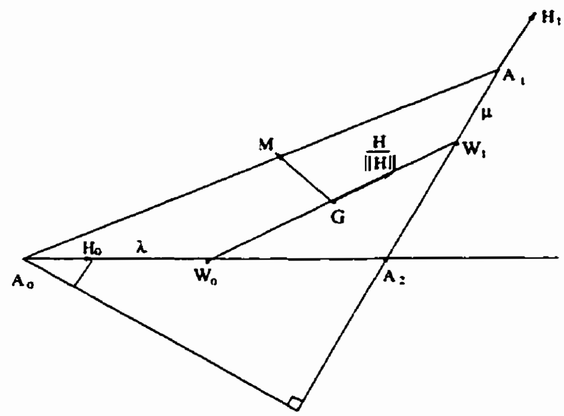

Figure 5.3: Triangle Construction

Use Eqn. (2.12), (2.13) and t varies from 0 to 1;

case cubic:

Use Eqns. (2.25) and t varies from 0 to 1;

case PH cubic:

Use Eqns. from (2.28) to (2.31) and t varies from 0 to 1;

case PH quintic:

Use Eqns. (2.36) and t varies from 0 to 1;

case clothoidal:

Use Eqn. (2.46) to generate t_1, $t_0 = 0$,

Use Eqn. (2.38) to generate parameter a;

case Archimedean:

Input t_0, t_1, a, m;

case Logarithmic:

Use Eqn. (2.62) to generate parameter k and t varies from 0 to θ;

}

Procedure EvalQ(t, spiral_data)

```
Switch (spiral) {
    case quadratic:
        Use Eqn. (4.1) to evaluate it;
    case cubic:
        Use Eqn. (4.4) to evaluate it;
    case PH cubic:
        Use Eqn. (4.7) to evaluate it;
    case PH quintic:
        Use Eqn. (4.10) to evaluate it;
    case clothoidal:
        Use Eqn. (4.13) to evaluate it;
    case Archimedean:
        Use Eqn. (4.18) to evaluate it;
    case Logarithmic:
        Use Eqn. (4.23) to evaluate it;
}
```

Procedure EvalDQ(t, spiral_data)

```
Switch (spiral) {
    case quadratic:
        Use Eqn. (4.2) to evaluate it;
    case cubic:
        Use Eqn. (4.5) to evaluate it;
    case PH cubic:
        Use Eqn. (4.8) to evaluate it;
```

case PH quintic:

Use Eqn. (4.11) to evaluate it;

case clothoidal:

Use Eqn. (4.14) to evaluate it;

case Archimedean:

Use Eqn. (4.19) to evaluate it;

case Logarithmic:

Use Eqn. (4.24) to evaluate it;

}

Procedure FindBiArcTri (t_0, t_1, spiral_data)

1. $\mathbf{A}_0 \longleftarrow EvalQ(t_0, spiral\_data)$; $\mathbf{A}_1 \longleftarrow EvalQ(t_1, spiral\_data)$;

2. $\mathbf{H}_0 \longleftarrow EvalDQ(t_0, spiral\_data)$; $\mathbf{H}_1 \longleftarrow EvalDQ(t_1, spiral\_data)$;

   Normalize $\mathbf{H}_0$, $\mathbf{H}_1$;

3. $\mathbf{H} \longleftarrow \mathbf{A}_1 - \mathbf{A}_0$;

4. $\mathbf{M} \longleftarrow (\mathbf{H} \cdot \mathbf{H}_1)\mathbf{H}_1 - \mathbf{H}$;

   Normalize $\mathbf{M}$; (Refer to Fig. 5.3)

5. $\mathbf{A}_2 \longleftarrow \mathbf{A}_0 + \frac{\mathbf{H}\cdot\mathbf{M}}{\mathbf{H}_0\cdot\mathbf{M}}\mathbf{H}_0$.

6. return $\mathbf{A}_0$, $\mathbf{A}_1$, $\mathbf{A}_2$, $\mathbf{H}_0$, $\mathbf{H}_1$, $\mathbf{H}$.

Procedure FitBiArc($\mathbf{H}_0$, $\mathbf{H}_1$, $\mathbf{H}$)

1. normalize $\mathbf{H}$.

2. $\sin\alpha \longleftarrow \mathbf{H}_0 \times \mathbf{H}$.

3. $\sin\beta \longleftarrow \mathbf{H} \times \mathbf{H}_1$.

4. According to *Lemma* 5.1,

$$\lambda \longleftarrow \frac{\sin(\beta)}{\sin(\alpha+\beta)+\sin(\beta)+\sin(\alpha)}$$

5.

$$\mu \longleftarrow \frac{\sin(\alpha)}{\sin(\alpha+\beta)+\sin(\beta)+\sin(\alpha)}$$

6. $\mathbf{W}_0 \longleftarrow \mathbf{A}_0 + \lambda\mathbf{H}_0$.

7. $\mathbf{G} \longleftarrow \mathbf{W}_0 + \lambda\mathbf{H}$.

8. $\mathbf{W}_1 \longleftarrow \mathbf{A}_1 - \mu\mathbf{H}_1$.

9. return $\mathbf{A}_0$, $\mathbf{W}_0$, $\mathbf{G}$, $\mathbf{W}_1$, $\mathbf{A}_1$.

Procedure FindArc(**A**,**W**,**G**)

1. $b \longleftarrow \| \mathbf{W} - \mathbf{A} \|$.

2. $c \longleftarrow \| \mathbf{G} - \mathbf{A} \|$.

3. The radius of the arc r: $r = \frac{bc}{\sqrt{4b^2-c^2}}$.

4. $\mathbf{N} \longleftarrow$ the unit normal of **AW**.

5. The centre of the circle $\mathbf{C} \longleftarrow \mathbf{A} + r\mathbf{N}$.

6. Degree of the arc $\longleftarrow \arctan \frac{(\mathbf{A}-\mathbf{C})\times(\mathbf{G}-\mathbf{C})}{(\mathbf{A}-\mathbf{C})\cdot(\mathbf{G}-\mathbf{C})}$

Procedure DevAtJoint ($\mathbf{H}$)

1. $f(t) \longleftarrow \{\mathbf{Q}(t) - \mathbf{G}\} \cdot \mathbf{H}$;

2. Use bisection method to solve $f(t) = 0$.

Procedure MaxDevP

1. Define $g : g(t) \longleftarrow$ Eqn. (3.7), where α depends on spirals:

   Switch (spiral) {

   case quadratic:

   Use Eqn. (4.3);

   case cubic:

   Use Eqn. (4.6);

   case PH cubic:

   Use Eqn. (4.9) ;

   case PH quintic:

   Use Eqn. (4.12);

   }

2. if $g(u_i) * g(\eta) < 0$ then

   use bisection to solve $g(t) = 0$.

   else

   no local maxima.

Procedure MaxDevNP

1. Define $g : g(t) \longleftarrow \{\mathbf{Q}(t) - \mathbf{C}_i\} \cdot \mathbf{Q}'(t)$, where $\mathbf{Q}(t)$ and $\mathbf{Q}'(t)$ depend on spirals:

   Switch (spiral) {

case clothoid:

Use Eqn. (4.13) and (4.14);

case Arcimedian:

Use Eqn. (4.18) and (4.19);

case logarithmic:

Use Eqn. (4.23) and (4.24);

}

2. Define g'

Switch (spiral) {

case clothoid:

Use Eqn. (4.17);

case Archimedean:

Use Eqn. (4.22);

case logarithmic:

Use Eqn. (4.27);

}

3. if $((t_i < \eta)$ AND $g'(t_i)g(\eta) < 0)$ OR $((t_i > \eta)$ AND $g'(t_i)g(\eta) > 0)$ then

use bisection to solve $g(t) = 0$.

else

no local maxima.

Procedure ApproxSpiral $(\mathbf{P}_0, \mathbf{T}_0, c, c_0\theta, t_0, t_1, \tau)$

STEP 1

Initialize parameter to generate *spiral_data*.

{Invoke InitParameter ($\mathbf{P}_0, \mathbf{T}_0, c, c_0, \theta, t_0, t_1$).}

STEP 2

Invoke EvalQ, EvalDQ to compute $\mathbf{A}_0 = \mathbf{Q}(t_0), \mathbf{A}_1 = \mathbf{Q}(t_1)$.

$\mathbf{H}_0 = \mathbf{Q}'(t_0)$ and $\mathbf{H}_1 = \mathbf{Q}'(t_1)$.

STEP 3

Determine $\mathbf{A}_2$ as the intersection of the straight lines parallel to $\mathbf{H}_0$ and $\mathbf{H}_1$ at $\mathbf{A}_0$ and $\mathbf{A}_1$, respectively.

{Invoke FindBiarcTri (t_0,t_1, spiral_data) }

STEP 4

Find the incentre, $\mathbf{G}$, of the triangle with vertices $\mathbf{A}_0, \mathbf{A}_2$ and $\mathbf{A}_1$.

{Invoke FitBiarc ($\mathbf{H}_0$, $\mathbf{H}_1$, $\mathbf{H}$) }

STEP 5

Find the centres, $\mathbf{C}_i$ and radii, r_i, of the biarc, joined at $\mathbf{G}$, and defined by the triangle with vertices $\mathbf{A}_0, \mathbf{A}_2$ and $\mathbf{A}_1$.

{Invoke FindArc ($\mathbf{A}_0$, $\mathbf{W}_0$, $\mathbf{G}$) and FindArc ($\mathbf{A}_1$, $\mathbf{W}_1$, $\mathbf{G}$)}

STEP 6

Use *Theorems* 3.1 and 3.2 to determine the maximum deviation, δ, of the biarc from the spiral along a radial direction of the biarc, and the value, η, of t for which it occurs.

{Invoke DevAtJoint to calculate the deviation at joint and MaxDevP, MaxDevNP to calculate the extrema if it appears in the interval.}

STEP 7

If $\delta < \tau$, then store the biarc,

otherwise

invoke ApproxSpiral $(\mathbf{P}_0, \mathbf{T}_0, c, c_0, \theta, t_0, \eta, \tau)$

and ApproxSpiral $(\mathbf{P}_0, \mathbf{T}_0, c, c_0, \theta, \eta, t_1, \tau)$

Chapter 6

Examples

The algorithm was tested on many examples. The results presented in this chapter are based on the following initial conditions. The beginning curvature is zero for cubic, PH cubic, PH quintic, clothoidal spiral segments. For the quadratic and cubic Bézier spiral segments, $\mathbf{P}_0 = (0,0)$, $\mathbf{T}_0 = (1,0)$, $\theta = 51.34°$, $c = 0.41574$. For PH cubic, PH quintic and clothoid spiral segment, $\mathbf{P}_0 = (0,0)$, $\mathbf{T}_0 = (1,0)$, $\theta = 135°$, the ending curvatures are 4,5 and 1.5 respectively. For Archimedean spiral segment, $\mathbf{P}_0 = (0,0)$, $a = 10$, $m = 2$, $t_0 = 0.01$, $t_1 = 0.2$. The parameter of logarithmic spiral segment is: $\mathbf{P}_0 = (0,0)$, $\mathbf{T}_0 = (1,0)$, $\theta = 135°$, $c_0 = 0.25$, $c = 4$.

Table (6.1) to (6.7) show the number of arcs needed for each spiral segment given a tolerance ranging from 0.1 to 0.00001 decreasing by a factor of 0.1.

The arc spline approximations using a specified tolerance of 0.001 are illustrated in Fig. (6.1) to (6.7). Scales indicate the units. The arc spline approximations are visually indistinguishable from the corresponding spiral segments.

Table (6.8) to (6.14) show the radii of the arcs needed for each spiral when the tolerance is equal to 0.001. Observe that they form a monotone decreasing sequence for each spiral segment.

Fig. (6.8) to Fig. (6.14) show the relationship between number of arcs and tolerance. The solid lines show the number of arcs for a given tolerance. The dotted lines show the actual deviation for the number of arcs used. So the solid line is always above the dotted line.

Table 6.1: Results of Approximation of Quadratic Bézier Spiral Segment

Specified tolerance, τ	Number of arcs	Maximum deviation
0.1	2	0.0274124
0.01	4	0.00573994
0.001	8	0.00097705
0.0001	16	0.00008590
0.00001	36	0.00000984

Table 6.2: Results of Approximation of Cubic Bézier Spiral Segment

Specified tolerance, τ	Number of arcs	Maximum deviation
0.1	4	0.01395
0.01	8	0.002306
0.001	12	0.0009584
0.0001	26	0.00009716
0.00001	54	0.00000785

Table 6.3: Results of Approximation of PH Cubic Spiral Segment

Specified tolerance, τ	Number of arcs	Maximum deviation
0.1	2	0.09257040
0.01	6	0.00641293
0.001	14	0.00095476
0.0001	28	0.00008077
0.00001	60	0.00000985

Table 6.4: Results of Approximation of PH Quintic Bézier Spiral

Specified tolerance, τ	Number of arcs	Maximum deviation
0.1	2	0.03537248
0.01	10	0.00517404
0.001	20	0.00059789
0.0001	36	0.00009287

Table 6.5: Results of Approximation of Clothoid Spiral Segment

Specified tolerance, τ	Number of arcs	Maximum deviation
0.1	4	0.01833951
0.01	8	0.00229056
0.001	14	0.00051891
0.0001	26	0.00009777
0.00001	74	0.00000969

Table 6.6: Results of Approximation of Archimedean Spiral Segment

Specified tolerance, τ	Number of arcs	Maximum deviation
0.1	2	0.01965815
0.01	4	0.00186291
0.001	8	0.00027817
0.0001	12	0.00009493
0.00001	28	0.00000998

Table 6.7: Results of Approximation of Logarithmic Spiral Segment

Specified tolerance, τ	Number of arcs	Maximum deviation
0.1	4	0.01541348
0.01	6	0.00623577
0.001	12	0.00075185
0.0001	26	0.00007173
0.00001	56	0.00000972

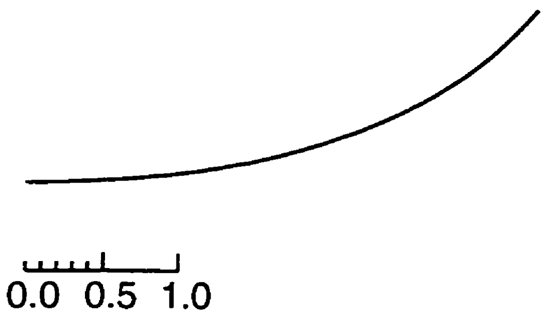

Figure 6.1: Arc Spline Approximation of Quadratic Bézier Spiral Segment

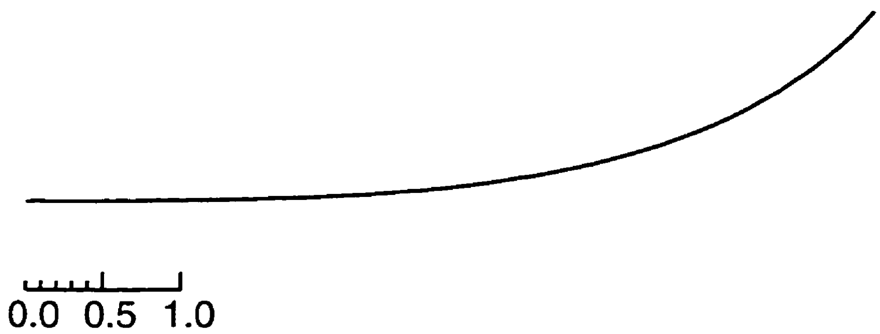

Figure 6.2: Arc Spline Approximation of Cubic Bézier Spiral Segment

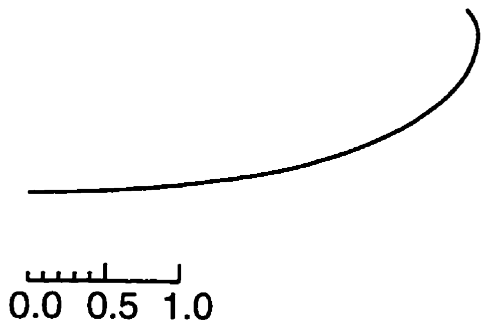

Figure 6.3: Arc Spline Approximation of PH Cubic Spiral Segment

Figure 6.4: Arc Spline Approximation of PH Quintic Spiral Segment

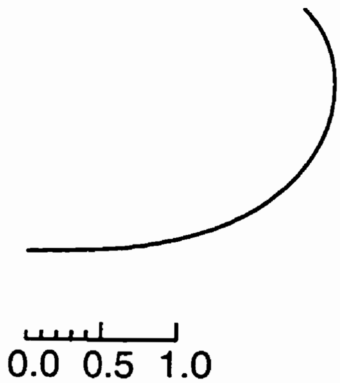

Figure 6.5: Arc Spline Approximation of Clothoid Segment

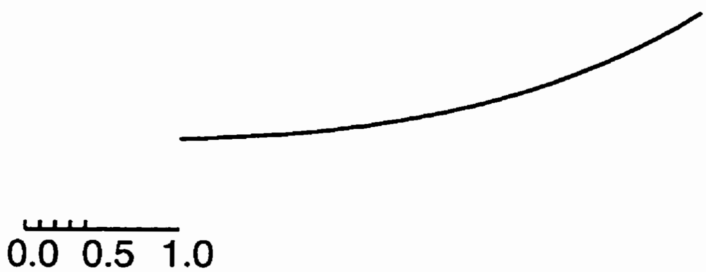

Figure 6.6: Arc Spline Approximation of Archimedean Segment

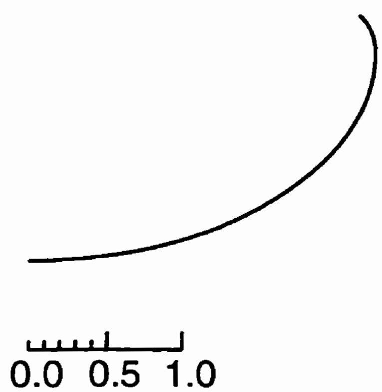

Figure 6.7: Arc Spline Approximation of Logarithmic Spiral Segment

Table 6.8: Radius of Approximation of Quadratic Bézier Spiral Segment by Arc Spline

sequence of biarcs	radius of left arc	radius of right arc
1	9.439	7.921
2	6.966	5.040
3	4.343	3.359
4	2.908	2.408

Table 6.9: Radius of Approximation of Cubic Bézier Spiral Segment by Arc Spline

sequence of biarcs	radius of left arc	radius of right arc
1	176.193	43.273
2	35.427	21.506
3	15.793	8.261
4	6.442	4.156
5	3.601	2.993
6	2.717	2.406

Table 6.10: Radius of Approximation of PH Cubic Spiral Segment by Arc Spline

sequence of biarcs	radius of left arc	radius of right arc
1	10.505	6.728
2	5.620	4.364
3	3.698	2.429
4	1.838	0.910
5	0.684	0.458
6	0.395	0.323
7	0.289	0.250

Table 6.11: Radius of Approximation of PH Quintic Spiral Segment by Arc Spline

sequence of biarcs	radius of left arc	radius of right arc
1	211.099	51.473
2	41.828	24.789
3	20.708	15.014
4	12.268	7.592
5	5.900	3.369
6	2.729	2.051
7	1.617	0.824
8	0.619	0.397
9	0.336	0.268
10	0.236	0.200

Table 6.12: Radius of Approximation of Clothoid Spiral Segment by Arc Spline

sequence of biarcs	radius of left arc	radius of right arc
1	21.681	5.429
2	4.517	2.895
3	2.530	2.020
4	1.796	1.417
5	1.259	1.003
6	0.933	0.844
7	0.792	0.687

Table 6.13: Radius of Approximation of Logarithmic Spiral Segment by Arc Spline

sequence of biarcs	radius of left arc	radius of right arc
1	3.741	2.773
2	2.440	2.017
3	1.769	1.223
4	1.023	0.734
5	0.636	0.512
6	0.440	0.284

Table 6.14: Radius of Approximation of Archimedean Spiral Segment by Arc Spline

sequence of biarcs	radius of left arc	radius of right arc
1	14.777	10.593
2	9.089	6.887
3	6,268	5.415
4	5.034	4.483

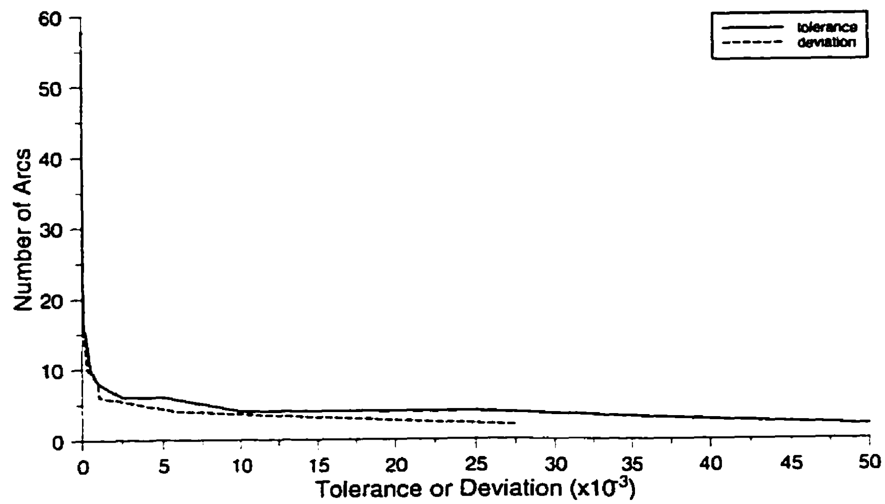

Figure 6.8: Quadratic Bézier Spiral

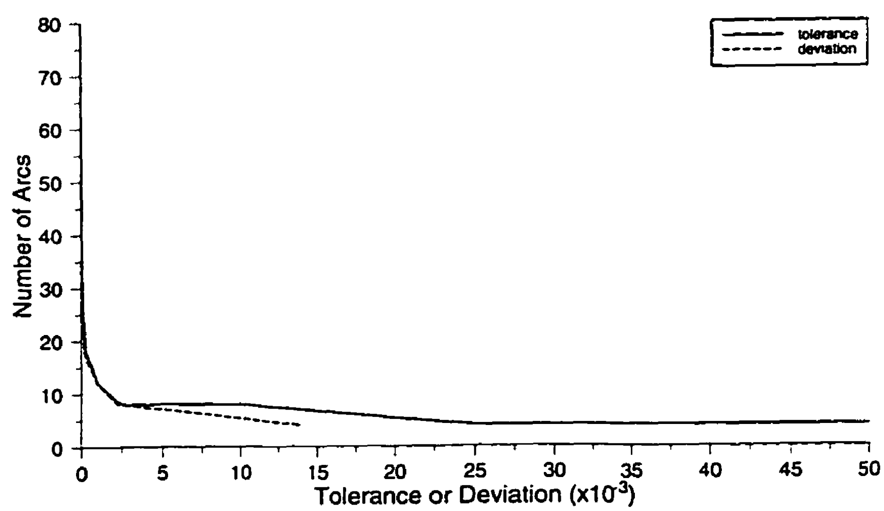

Figure 6.9: Cubic Bézier Spiral

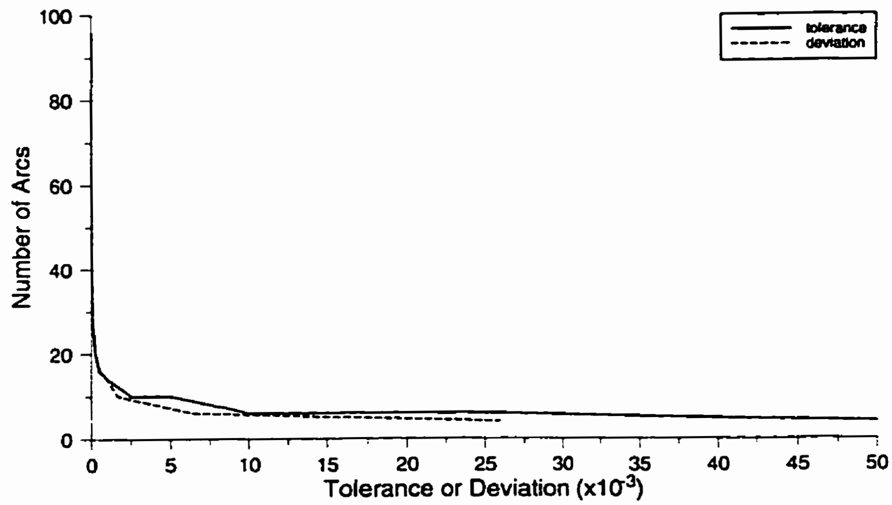

Figure 6.10: PH Cubic Bézier Spiral

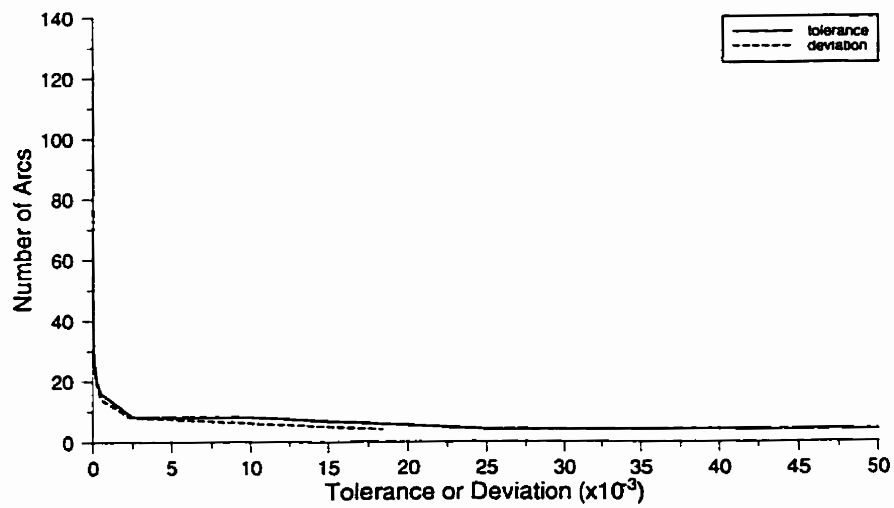

Figure 6.11: PH Quintic Bézier Spiral

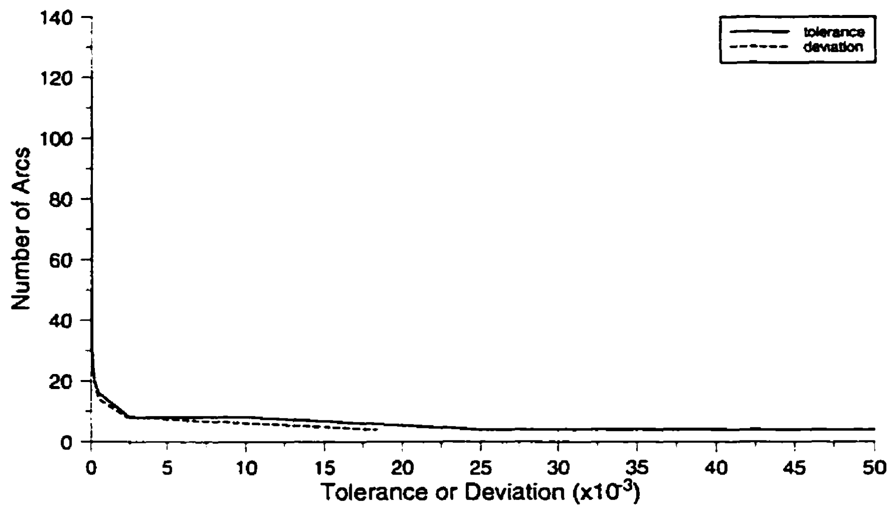

Figure 6.12: Clothoidal Spiral

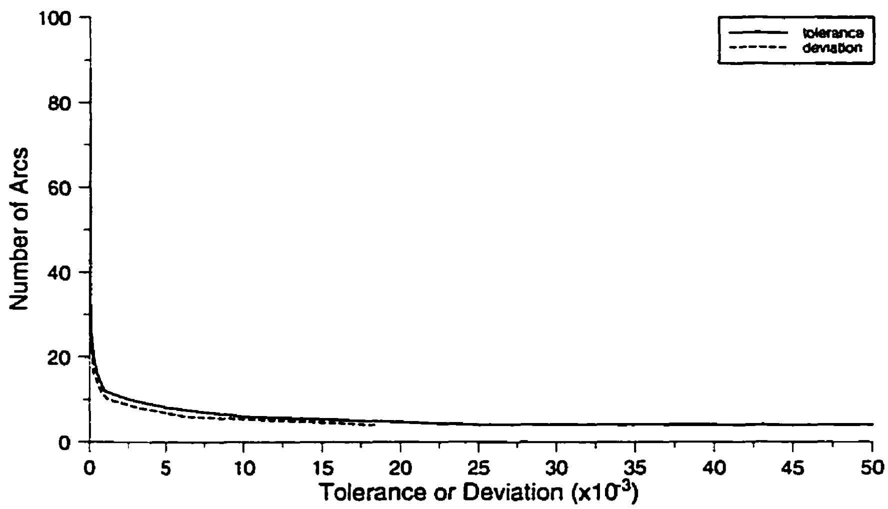

Figure 6.13: Logarithmic Spiral

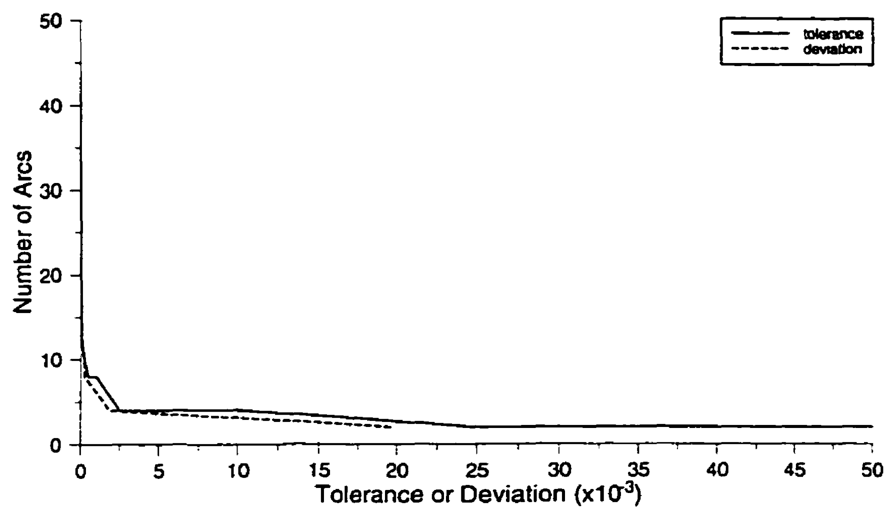

Figure 6.14: Archimedean Spiral

Chapter 7

Conclusions

In this thesis, a method for approximating spiral segments is proposed. To approximate all kinds of spirals, this method can be applied by approximating each subpart separately after subdividing the spiral to subparts appropriately. Seven kinds of spiral segment namely quadratic Bézier, cubic Bézier, PH cubic, PH quintic, clothoid, Archimedean, logarithmic were examined. Accuracy can be achieved by designating a specific tolerance. The method were tested on all of these spirals. Following are some concluding observations.

7.1 Tendency of the Radius

For tolerance 0.001, observe the radii of arc splines using the same parameters and the results are recorded in Tables (6.8) to (6.14). The arcs are listed in the order of increasing parameter t. The "left" arc is the one which approximates a part of the spiral with smaller curvature in a triangle construction while the "right" arc is the other arc. From the radii traced, it seems that radii get smaller when a winding spiral segment is approximated by using this biarc method.

7.2 Relationship between Number of Arcs and Tolerance

Fig.(7.1) shows a logarithmic plot of deviation versus number of arcs for a spline approximation of various spiral segments. For the y-axis, $y = \log_{10}(deviation)$, for the x-axis, $x = \log_{10}(number\ of\ arcs)$. The plots are close to a straight line whose slope is -3. Suppose d denotes the deviation, n denotes the number of arcs and C is a constant. From Fig. (7.1),

$$\log d \approx -3 \log n + C$$

$$\log d \approx \log(Cn^{-3})$$

$$d \approx Cn^{-3}$$

$$d \approx \mathbf{O}(n^{-3}).$$

In another word, the error of approximation seems to be $\mathbf{O}(n^{-3})$ which is consistent with the result of [MW95].

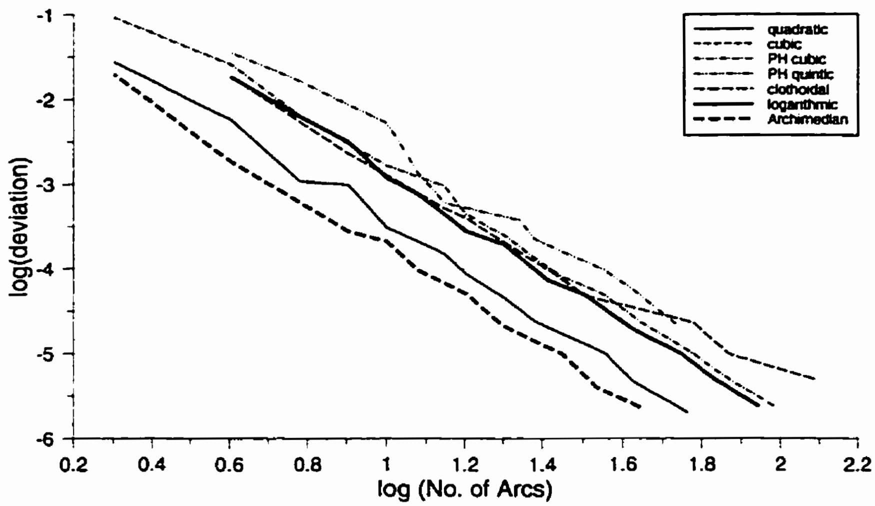

Figure 7.1: Logarithmic Pact of Deviation vs. No. of Arcs

Bibliography

[Ada69] R.K. Adair. *Concepts in Physics.* Academic Press, New York, 1969.

[Baa84] K.G. Baass. The Use of Clothoid Templates in Highway Design. *Transportation Forum*, (1-3):47–52, 1984.

[BBB87] R.H. Bartel, J.C. Beatty, and B.A. Barsky. *An Introduction to Splines for Use in Computer Graphics and Geometric Modelling.* Morgan Kaufmann, Los Altos.CA, 1987.

[BF97] C. Baumgarten and G. Farin. Approximation of Logarithmic Spirals. *Computer Aided Geometric Design*, (14):515–532, 1997.

[Boe60] J. Boersma. Computation of Fresnel Integrals. *Mathematics of Computation*, 14:380, 1960.

[Bol75] K.M. Bolton. Biarc Curves. *Computer-Aided Design*, 7:89–92, 1975.

[Cox42] H.S.M. Coxeter. *Non-euclidean Geometry.* The University of Toronto Press, Toronto, Canada, 1942.

[Cox61] H.S.M. Coxeter. *Introduction to Geometry.* Johm Wiley and Sons, Inc., New York, London, 1961.

[dC76] Manfredo P. do Carmo. Differential geometry of curves and surfaces. 1976.

[Far93] G. Farin. *Curves and Surfaces for Computer Aided Geometric Design: A Practical Guide.* Academic Press, San Diego, 1993. Third Edition.

[Far94] R.T. Farouki. The conformal map $z \rightarrow z^2$. *Computer Aided Geometric Design*, 11:363–390, 1994.

[FS90] R.T. Farouki and T. Sakkalis. Pythagorean Hodograph. *IBM J. Res. and Develop.*, 34:736–752, 1990.

[Gug63] H.W. Guggenheimer. *Differential Geometry.* McGraw-Hill, New York, 1963.

[Hea85] M. A. Heald. Rational Approximations for the Fresnel Integrals. *Mathematics of Computation*, 44(170):459–461, April,1985.

[Hic67] T.F. Hickerson. *Route Location and Design.* McGraw-Hill Book Company, U. S. A., 1967.

[HL93] J. Hoschek and D. Lasser. *Foudamentals of Computer Aided Geometric Design.* A K Peters, Wellesley,Massachusetts, 1993. Translated from German by L.L. Schumaker.

[Meh74] E. Mehlum. Nonlinear Splines, in: R.E. Barnhill and R.F.Reisenfeld, Eds. *Computer Aided Geometric Design(Academic Press, London)*, pages 173–205, 1974.

[Mor92] Christopher Morris. *Academic Press Dictionary of Science and Technology*. Harcourt Brace Jovanovich Publishers, New York, London, San Diego, Boston, 1992.

[MP84] K. Marciniak and B. Putz. Approximation of Spirals by Piecewise Curves of Fewest Circular Arc Segments. *Computer-Aided Design*, 16(2):87–90, 1984.

[MW89] D.S. Meek and D.J. Walton. The Use of Cornu Spirals in Drawing Planar Curves of Controlled Curvature. *Journal of Computational and Applied Mathematics*, 25:69–78, 1989.

[MW95] D.S. Meek and D.J. Walton. Approximation Smooth Planar Curves by Arc Splines. *Journal of Computational and Applied Mathematics*, 59:221–231, 1995.

[Pie86] L. Piegl. Curve Fitting Algorithm for Rough Cutting. *Computer-Aided Design*, 18:79–82, 1986.

[Sab77] M.A. Sabin. The Use of Piecewise Forms for the Numerical Representation of Shape. Technical Report 60, Comput. Automation Inst., Hungarian Acad. Sci., 1977.

[Sch96] P.R. Schmitt. Reactive Path Shaping: Local Path Planning for Autonomous Mobile Robots in Aisles, 1996.

[vS90] D.H. von Seggern. *CRC Handbook of Mathematical Curves and Surfaces*. CRC Press, Inc., Boca Raton, Florida, 1990.

[WM] D.J. Walton and D.S. Meek. G^2 Curves Composed of Planar Cubic and Pythagorean Hodograph Quintic Spirals. *Computer Aided Geometric Design.* in press.

[WM94] D.J. Walton and D.S. Meek. Approximation of Quadratic Bézier Spiral by Arc Splines. *Journal of Computational and Applied Mathematics*, (54):107–120, 1994.

[WM96a] D.J. Walton and D.S. Meek. A Planar Cubic Bézier Spiral. *Journal of Computational and Applied Mathematics*, (72):85–100, 1996.

[WM96b] D.J. Walton and D.S. Meek. A Pythagorean Hodograph Quintic Spiral. *Computer-Aided Design*, (28):943–950, 1996.

[WM96c] D.J. Walton and D.S. Meek. Approximation of a Planar Cubic Bézier Spiral by Circular Arcs. *Journal of Computational and Applied Mathematics*, (75):47–56, 1996.

[WX91] D.J. Walton and R. Xu. Turning Point preserving Planar Interpolation. *ACM Transactions on Graphics*, 10(3):297–311, 1991.

[Yat52] R.C. Yates. *Curves and Their Properties.* The National Council of Teachers of Mathematics, U. S. A., 1952.

[YW94] M.K. Yeung and D.J. Walton. Curve Fitting with Arc Splines for NC Tool Path Generation. *Computer-Aided Design*, 26(11):845–849, 1994.

IMAGE EVALUATION TEST TARGET (QA-3)

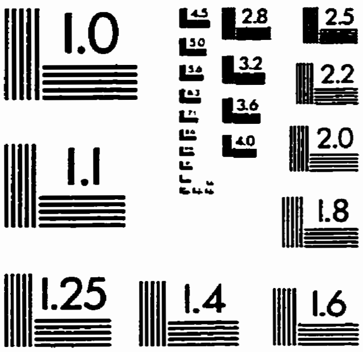

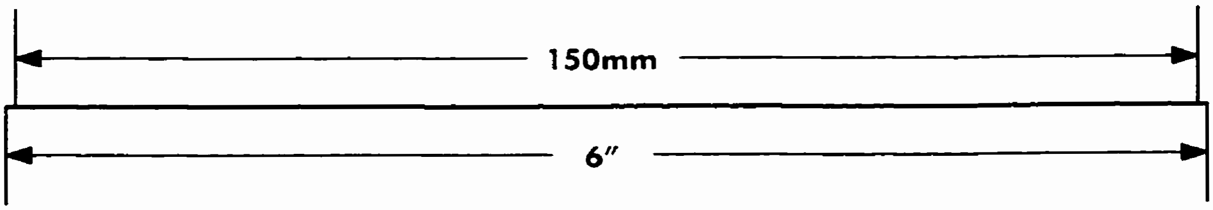

APPLIED IMAGE . Inc
1653 East Main Street
Rochester, NY 14609 USA
Phone: 716/482-0300
Fax: 716/288-5989